The role of sea surface temperature in the atmospheric seasonal cycle of the equatorial Atlantic

Lander R. Crespo, Noel Keenlyside & Shunya Koseki
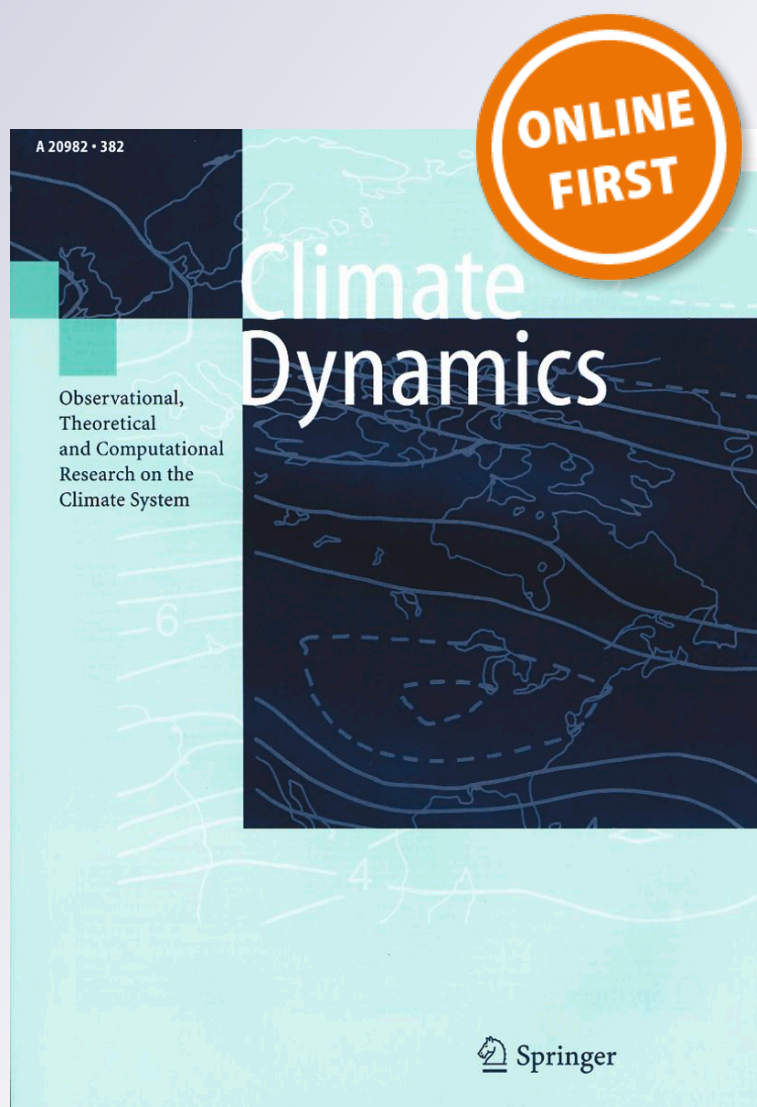
A 20982 · 382

Climate Dynamics

Observational,
Theoretical
and Computational
Research on the
Climate System

ONLINE FIRST

6

4   4

⌂ Springer

⌂ Springer

Springer

CrossMark

The role of sea surface temperature in the atmospheric seasonal cycle of the equatorial Atlantic

Lander R. Crespo[1] · Noel Keenlyside[1] · Shunya Koseki[1]

Abstract
We investigate the role of sea surface temperature (SST) and land surface temperature (LST) in driving the seasonal cycle of the atmosphere (surface winds and precipitation) in the tropical Atlantic. For this we compare three atmospheric general circulation model (AGCM) experiments for the historical period 1982–2013 forced by different SST: (1) observed daily-climatological SST, (2) globally annual-mean SST, and (3) annual-mean SST in the equatorial Atlantic and daily-climatological SST elsewhere. Seasonal variations in SST strongly influence the seasonal evolution of the West African Monsoon (WAM) and ITCZ over the equatorial Atlantic Ocean. Forcing the model with annual mean SST (globally and in the equatorial Atlantic) considerably reduces the seasonal variance in the atmosphere, except for the zonal winds in the eastern equatorial Atlantic. Equatorial Atlantic SST contributes to the seasonal cycle in precipitation and meridional winds over the entire equatorial Atlantic, but only strongly influences zonal winds in the western equatorial Atlantic and has little influence on the northward penetration of the WAM. The leading modes of coupled SST–LST-atmosphere co-variability are identified by multivariate analysis. The analysis shows that both LST and SST drive seasonal variations in precipitation over equatorial Atlantic, with the LST being a larger contributor to the continental rainfall in West Africa. The coupling between ocean and atmosphere is stronger in the western than in the eastern equatorial Atlantic. The pressure adjustment mechanism is the main driver of the surface meridional wind convergence in the eastern tropical Atlantic.

Keywords Equatorial Atlantic · ITCZ · WAM · Seasonal cycle · AGCM

1 Introduction

The Intertropical Convergence Zone (ITCZ) is a band of tropical deep-convection that can be identified as the maximum in time-mean precipitation, and by the convergence of surface winds from both hemispheres. In the climatological mean the ITCZ sits north of the equator in the Atlantic. The ITCZ movement in the Atlantic is not symmetric about the equator and does not follow the insolation maximum, but it exhibits an annual cycle in the eastern tropical Atlantic (see Fig. 1). The sea surface temperature (SST) in the eastern equatorial Atlantic and the surface wind convergence onto the ITCZ, also show an annual cycle, in contrast to the semiannual cycle present in the insolation at the top of

the atmosphere (Mitchell and Wallace 1992; Wallace et al. 1989). The ITCZ location is influenced by SST patterns, with warmer SSTs favouring deep convection, and thus determining the surface wind patterns. However, it is still not fully understood how the SST, winds and ITCZ interact to form the tropical Atlantic climatology.

The determination of the annual mean position of the Atlantic ITCZ implicates various processes. Philander et al. (1996) proposed local ocean–atmosphere interactions and continental asymmetries as the main factors determining the annual mean position of the ITCZ north of the equator. The shallower thermocline induced by prevailing easterly winds in eastern Atlantic, favours ocean–atmosphere interaction since the surface winds can affect the SST in this region more strongly. The shape of the continents, in particular the bulge of western Africa to the north of the Gulf of Guinea is a determinant factor that can explain why the Northern Hemisphere favours warmer SST and why the ITCZ is located north of the equator in the Atlantic. Other studies (Kang et al. 2008, 2009; Frierson and Hwang 2012)

✉ Lander R. Crespo
  lander.crespo@uib.no

1 Geophysical Institute, University of Bergen and Bjerknes Centre for Climate Research, Postboks 7803, 5020 Bergen, Norway
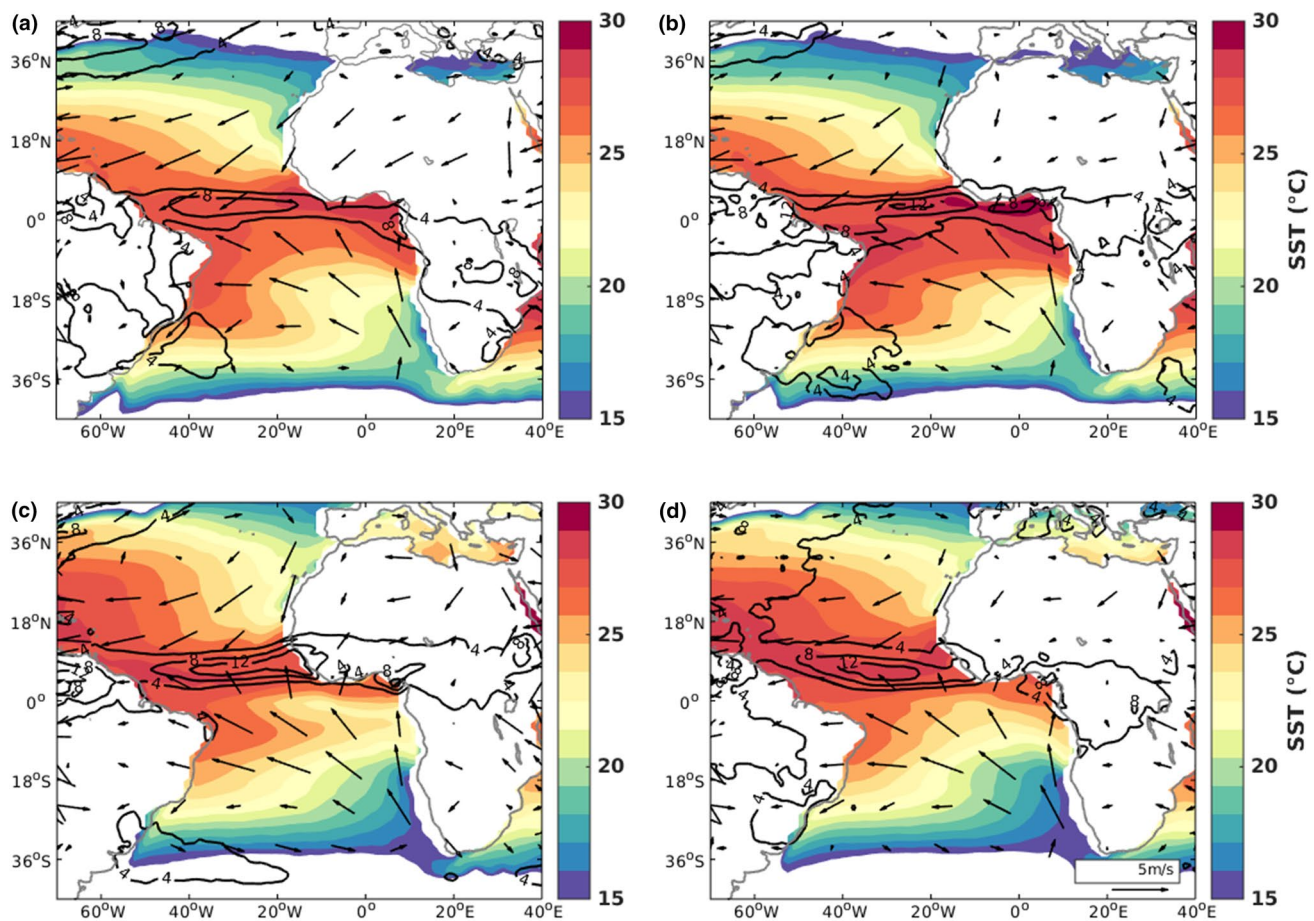
Fig. 1 Observed climatology of SST in °C, precipitation in mm and surface winds in m/s for the different seasons based on optimum interpolation sea surface temperature (OISST), tropical rainfall meas-uring mission (TRMM) and the Japanese 55-year Reanalysis (JRA-55) datasets, respectively. We show the SST in shading, the precipita-tion in contours and the winds in vectors

suggest that the position of the ITCZ is determined by extra-tropical interhemispheric differential heating. Consistently, Mechoso et al. (2016) found extratropical SSTs over the Southern Ocean to be an important trigger of the northern location of the ITCZ. The impact of remotely driven changes in the Hadley circulation is strongly counteracted by the local wind-driven circulation (Green and Marshall 2017). Contrastingly, Zhang and Delworth (2005) showed that the Atlantic Meridional Overturning Circulation (AMOC) con-trols the annual mean position of the ITCZ in the tropical Atlantic with a weakening of the oceanic overturning circu-lation resulting in a southward shift of the ITCZ. To main-tain the energetic balance, the net atmospheric and oceanic heat transport has to be zero at the equator. Since the oceanic heat transport is northward at the equator due to the AMOC (Lumpkin and Speer 2007), the atmosphere transports heat southward across the equator in order to keep the energy balance. The atmosphere achieves this by situating the ITCZ north of the equator (Schneider et al. 2014; Marshall et al. 2014).

As for the annual mean, local and large-scale processes also control the seasonal evolution of the ITCZ and atmos-pheric circulation. The seasonal cycle in the equatorial Atlantic is particularly interesting because of the competing roles of ocean and land. The observed seasonal variations in SST, precipitation and surface winds reveal a tight rela-tion between ocean and atmosphere in the tropical Atlantic (Fig. 1). During boreal winter (DJF) the precipitation sits close to the equator over the area where the SST is maximum and where the northern and southern hemisphere winds con-verge. The seasonal cycle of the SST is characterized by a rapid cooling from April to July, caused by stronger south-easterly winds close to the equator. These winds produce upwelling (downwelling) and elevate (deepen) the thermo-cline to the south (north) of the equator. This intensifies the contrast between warm waters north of the equator, and cold waters south and at the equator (Moore et al. 1978). The minimum in the SST along the Gulf of Guinea—known as the Atlantic Cold Tongue (ACT)—lasts the whole boreal summer (JJA). This creates a strong temperature gradient

between ocean and land, and it is associated with a strengthening of the southerly winds. The seasonal ACT and the intensified winds coincide with the northward migration of the rainband away from the equator onto the West African continent, with intense precipitation reaching as far north as 15°N in boreal summer.

The seasonal evolution of the ITCZ is largely determined by differential hemispheric heating. The extratropical seasonal cooling and heating of the hemispheres shift the ITCZ towards the warmer hemisphere (Kang et al. 2009), thus moving northward (southward) in summer (winter) (here we refer to the Northern Hemisphere seasons). Li and Philander (1997) (LP97 hereafter) suggest that seasonal changes in the eastern tropical Atlantic SST are the passive response of the ocean to the seasonal changes in the winds, which in turn are mainly driven by the changes in land temperatures, and that local air–sea interactions play a minor role. Other studies suggest that the annual cycle of SST is a product of ocean–atmosphere interactions (Okumura and Xie 2004; Druyan and Fulakeza 2015; Meynadier et al. 2016; Diakhaté et al. 2018). Okumura and Xie (2004) (OX04 hereafter) showed that the ACT intensifies the southerly winds in the Gulf of Guinea, and these push the rainband farther north over the land. Supporting this, other modelling (Meynadier et al. 2016) and diagnostic (Diakhaté et al. 2018) studies found meridional SST and SLP gradients, and meridional winds over the Gulf of Guinea to be tightly related. In contrast, the regional modelling study of Druyan and Fulakeza (2015) suggested that the development of the ACT had little impact on the development of the West African summer Monsoon (WAM), but found an impact on its strength. While the impact of the continental WAM on ocean surface winds contributes to the cooling in the SST, the importance of the SST cooling for the development of the monsoonal winds, and subsequently, the precipitation is debated.

There is agreement that ocean–atmosphere interactions are important for the seasonal cycle of the ITCZ, the surface winds, and the SST over the western equatorial Atlantic. In particular, both LP97 and OX04 found a strong dependence of the seasonal cycle of surface winds in this region on the underlying SST. Furthermore, observational and modelling studies indicate that year-to-year variations in the ACT strongly influence the rainfall and the winds in the western equatorial Atlantic (Zebiak 1993; Chang et al. 2000; Keenlyside and Latif 2007; Richter et al. 2014). Diagnostic analysis indicates that the surface wind convergence in this region is not closely related to the underlying SST and SLP gradients, and rather related to convective heating anomalies (Richter et al. 2014; Diakhaté et al. 2018).

The present study investigates the role of the atmosphere–land–ocean interactions in driving the seasonal cycle of the atmosphere in the tropical Atlantic basin, with a special focus on the impact of the SST in the eastern Atlantic,

where the WAM dominates the annual variability in the atmosphere. We perform a series of sensitivity experiments with an atmospheric general circulation model (AGCM) to identify the impact of the SST on the seasonal variability of the atmosphere. We use different statistical techniques to carry out an objective quantification of the impact of SST and land surface temperature (LST) on the seasonal cycle of the low-level atmospheric circulation and deep convection. We find the main covariability ocean–atmosphere coupled mode related to the equatorial SSTs variability in the tropical Atlantic using Maximum Covariance Analysis (MCA). We also identify a dynamical mechanism that can explain the impact of the SST gradients on surface wind convergence, and subsequently deep convection, in the central and eastern equatorial Atlantic.

Section 2 describes the AGCM, the experimental design, and the datasets used. In Sect. 3 we summarise the two statistical techniques we use: (1) statistical verification and (2) a coupled field multivariate analysis. We present and discuss our main findings in Sect. 4 and summarize our conclusions in Sect. 5.

2 Data, model, and experimental design

2.1 Data and AGCM simulations

The following observational based products are used to characterise the observed seasonal cycle: Japanese 55-year Reanalysis (JRA-55, Kobayashi et al. 2015) dataset at a $1.25° × 1.25°$ horizontal resolution with daily time resolution; Tropical Rainfall Measurement Mission 3B42 (TRMM, Huffman et al. 2007) daily data with horizontal $0.25° × 0.25°$ resolution; and the National Oceanic and Atmospheric Administration (NOAA) Optimal Interpolated Sea Surface Temperature (OISST, Reynolds et al. 2007) dataset. We calculate the monthly climatological averages for the period 1982–2013 (except for TRMM that the period is 1998–2012) to characterise the seasonal cycle.

We conduct numerical simulations with the version 4.0 of the Community Atmospheric Model (CAM4) (Neale et al. 2013), which is a low-top global finite-volume gridded AGCM developed by the National Center for Atmospheric Research (NCAR). The model is integrated with the standard $0.9° × 1.25°$ horizontal resolution and 26 vertical layers (from the surface up to 5 hPa). The deep convection parameterization in CAM4 is based upon the bulk mass-flux scheme of Zhang and McFarlane (1995).

The model is forced with realistically varying solar radiation, and with different prescribed SSTs, which are derived from the OISST. This model also requires the prescription of the sea ice coverage (SIC), which is set to be the

observed fully varying field provided with the OISST in all experiments.

We carry out three numerical simulations for the period 1982–2013, in order to understand the impact of the seasonal cycle of the tropical Atlantic SST on the atmosphere. In the control run (**climSST**), daily mean climatological observed SSTs are prescribed globally, so that the interannual variability of SST is removed while the seasonal cycles of both land and ocean are retained. In the second run (**meanSST**), the model is forced with annual mean observed SSTs prescribed globally; hence, the insolation over the land is the only time-varying surface driver of the atmosphere relevant here. In the third run (**eqmeanSST**), annual mean observed SSTs are prescribed in the equatorial Atlantic (10S-5N, 70W-20E), and observed climatological SSTs are prescribed elsewhere; with this experiment we can investigate the role of the ocean variability in the equatorial Atlantic Ocean. We also performed a fourth historical simulation where the AGCM is forced by realistic SSTs including inter-annual variability, but the comparison of the resultant fields show that interannual variability of the SST does not greatly affect the seasonal

cycle of the atmosphere (not shown), so we do not consider this experiment further.

The seasonal cycle of the simulated atmospheric fields is calculated as the monthly averaged daily climatology of the corresponding period of 32 years. Our analysis focuses on three fields representative of the low-level atmospheric quantities associated with WAM: zonal and meridional surface winds, and total precipitation (hereafter, **U**, **V** and **PRECT**, respectively) in the tropical Atlantic basin. We also separately analyse the western (WEA, 4°S–4°N, 40°–20°W) and eastern (EEA, 4°S–4°N, 16°W–4°E) equatorial Atlantic regions.

2.2 Model performance in representing the tropical Atlantic climate

The model represents reasonably well the seasonal cycle of both precipitation and surface winds (Fig. 2), although our model tends to underestimate the amplitude of the zonal winds in the subtropics, where a stronger easterly component is evident. The equatorial region shows a higher agreement than the subtropics in surface winds, but the differences of
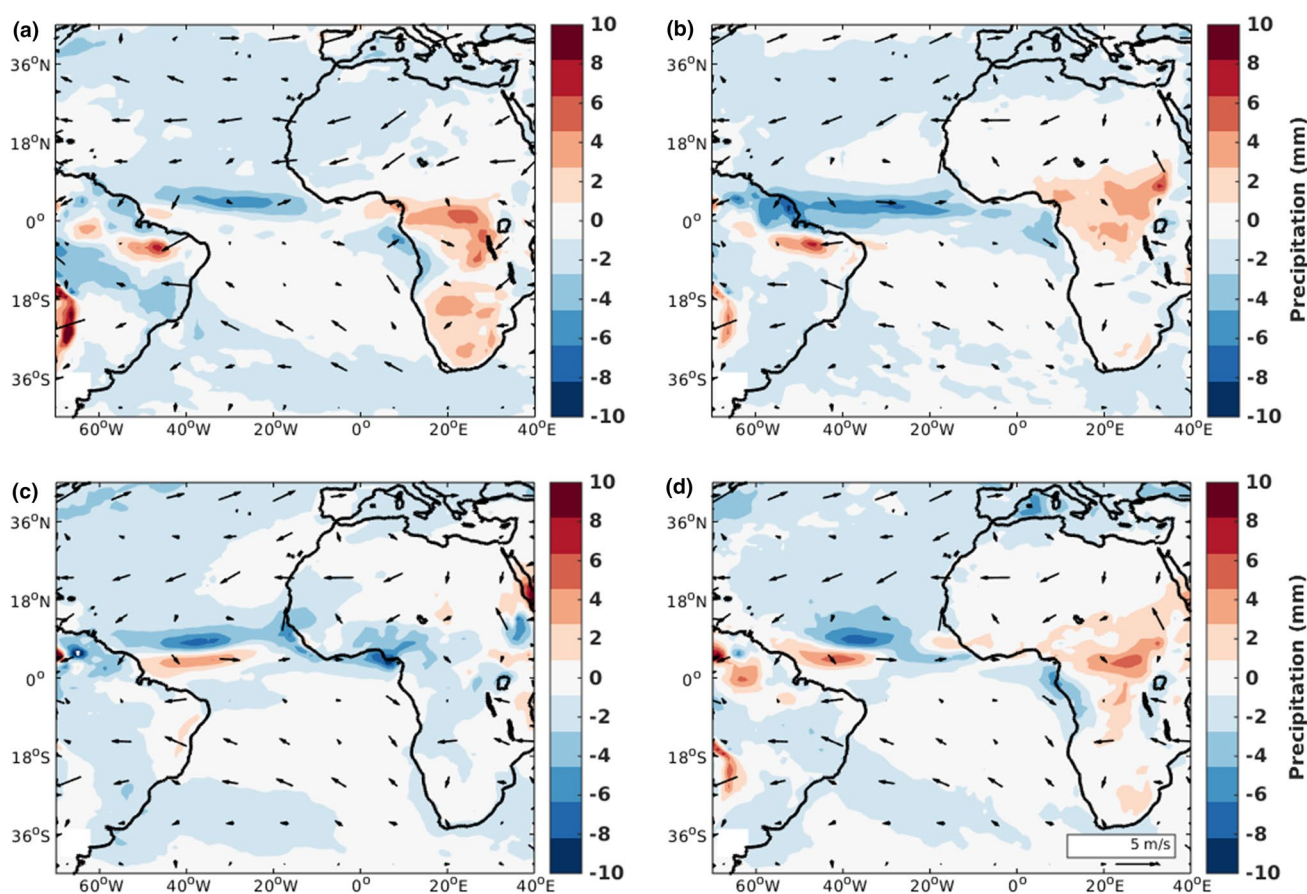

Fig. 2 Differences in rainfall in mm (shading) and surface winds in m/s (vectors) between climSST and TRMM dataset and between climSST and JRA dataset by seasons. Negative (positive) differences in rainfall are represented with blue (red) colors

surface winds between the model and the observations are still substantial (Fig. 2) along the equator. The model shows less precipitation than observations along most of the equatorial Atlantic probably associated with the errors in the representation of the surface winds (Fig. 2). There is a positive (negative) bias in zonal (meridional) winds over Angola coastal region in the southeastern Atlantic (e.g., Koseki et al. 2017). The monsoon region experiences stronger westerly and southerly winds in the annual average with respect to the observations; this might be related with the wet bias seen over west African continent.

The above enumerated biases are not only present in our model, but are common to most AGCMs (Richter 2015). Our study focuses on the equatorial Atlantic ocean and its surroundings, which we define as the region 70W–40E, and 15S–15N. In this region the errors of the model in simulating the surface winds are rather small, and in any season smaller than 20% of the actual observed value (Figs. 1, 2). The discrepancies in the precipitation compared to the observations (Figs. 1, 2), though, are larger, which is also a common issue present in many different GCMs (Mohino et al. 2011). The simulated and observed seasonal cycles of precipitation are strongly correlated (Fig. 3b) and the largest contribution to the mean squarre error (MSE) (Fig. 3c) with respect to the observations comes from the annual mean differences (Fig. 3a). Thus, the model captures really well the seasonality of the observations and hence is a suitable tool for investigating the seasonal cycle in the tropical Atlantic.

3 Statistical methodology

3.1 Verification of the joint distribution

We quantify the differences between datasets using a method analogous to the well-known forecast verification (Wilks 2011). Forecast verification is based, in general, on the study of the properties of the joint distribution function formed by the predictions and observations (Murphy and Winkler 1987). Here we perform three different verifications: (1) climSST run—observations, (2) meanSST run—climSST run and (3) eqmeanSST run—climSST run. In the first case, we evaluate the AGCM-ability to simulate the observations. In the second and third cases the joint distribution is formed from the model output values of each experiment. This provides an objective assessment of the agreement between simulations with alterned boundary conditions. The following statistical scores are used: standard deviation, the mean error (ME) or bias, the Pearson correlation coefficient, and the mean square error (MSE). Since we are interested in the seasonal cycle, all the indices are calculated for just 12 points in time corresponding to each month of the year. "Appendix" further describes the methodology. The results of these statistical analyses will be shown in Sect. 4.2. Note that the error in the model-to-model verification is interpreted as the difference between two sensitivity experiments.

3.2 Maximum covariance analysis

Maximum covariance analysis (MCA) or singular value decomposition (SVD) is a commonly used technique to identify a coherent temporal-spatial variability between two different fields. The method is based on the calculation of the principal vectors (pairs of empirical orthogonal functions, EOFs) that maximize the covariance between the two different fields and account for the largest fraction of the cross-covariance between the two jointly analyzed variables (Bjornsson and Venegas 1997) (see "Appendix" for a detailed explanation of the method).

We apply the MCA to three different cases to find the covariability patterns between ocean–atmosphere and between land–atmosphere. This way we identify the impact of land and ocean surface temperatures onto the atmosphere separately, and the mechanisms leading the spatial patterns of the coupled variability. In climSST-meanSST case, we apply the MCA to the difference between climSST and meanSST experiments using the SST as the predictor and the atmospheric variables U, V and PRECT as the predictands. This way we can identify the spatial patterns related with the influence of the ocean seasonal variability on the
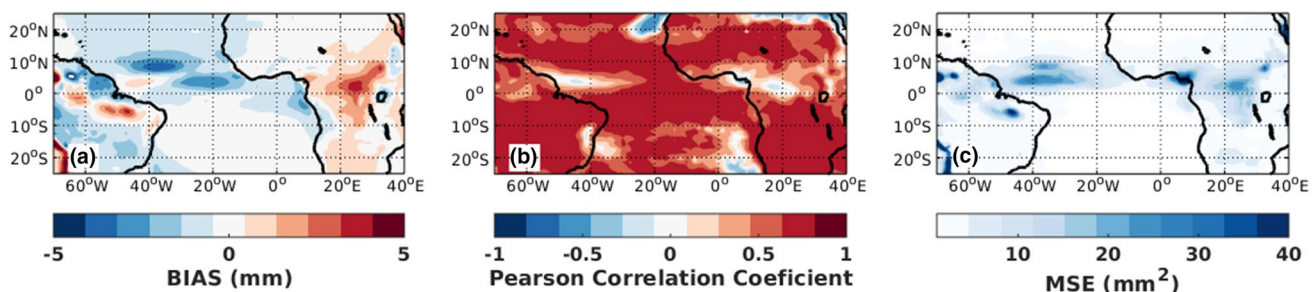

Fig. 3 Statistical indices accounting for the skill of our model. **a** Bias, **b** correlation and **c** MSE are shown for simulated precipitation from climSST run against TRMM dataset

atmosphere. In meanSST case, we perform the MCA of the meanSST experiment using the LST as the new predictor, and the same atmospheric variables as predictands. Thus, in this case, we can isolate the covariability between LST and the atmosphere when the annual cycle of SST is eliminated. The whole tropical Atlantic (30S–30N, 70W–20E) basin is considered for the first two cases. A third case, climSST-eqmeanSST, is presented where we analyze the coupled field patterns for the difference between climSST and eqmeanSST, using SST as the predictor against the atmospheric variables and focusing only in the equatorial Atlantic region (10S–5N, 70W–20E), since the difference of the SSTs is zero elsewhere. In this last case we only capture the covariability patterns between equatorial Atlantic SST and the tropical atmosphere. We will present the results of the statistical analysis with this methodology in Sect. 4.3.

The MCA is computed using the 12 month climatologies (and differences) computed from the runs. MCA requires a sufficient number of points to be efficient. Although we only have 12 points in time we find that the size of the grid is big enough and the annual cycle in the tropics dominant enough to build a cross-covariance matrix large enough for producing statistically reliable results.

4 Results

4.1 Simulation of the seasonal cycle

In this subsection, we show the difference in the seasonal cycle of the simulated atmospheric variables between climSST, meanSST and eqmeanSST runs to survey the impacts of global and equatorial Atlantic SST seasonal cycle on the atmosphere over the equatorial Atlantic.

In the western equatorial Atlantic (WEA) the observed zonal wind exhibits an annual cycle peaking in March to April, while in the eastern equatorial Atlantic (EEA) the annual cycle is dominated by a semiannual cycle peaking in February to March and September (Fig. 4). The meridional wind shows an annual cycle in both regions. Removing the annual cycle in the global SST (meanSST) reduces drastically the seasonal variability of surface winds in WEA, while in EEA the meridional component still exhibits a pronounced annual cycle because of the major role of the monsoon in that region. However, the abrupt jump of the meridional wind in spring associated with the onset of WAM is missed in the meanSST run. On the other hand, the zonal wind over EEA shows a very similar semiannual cycle for the climSST and meanSST runs, but it is weaker in meanSST. This indicates that neither the WAM nor the seasonality of SST play a role in the
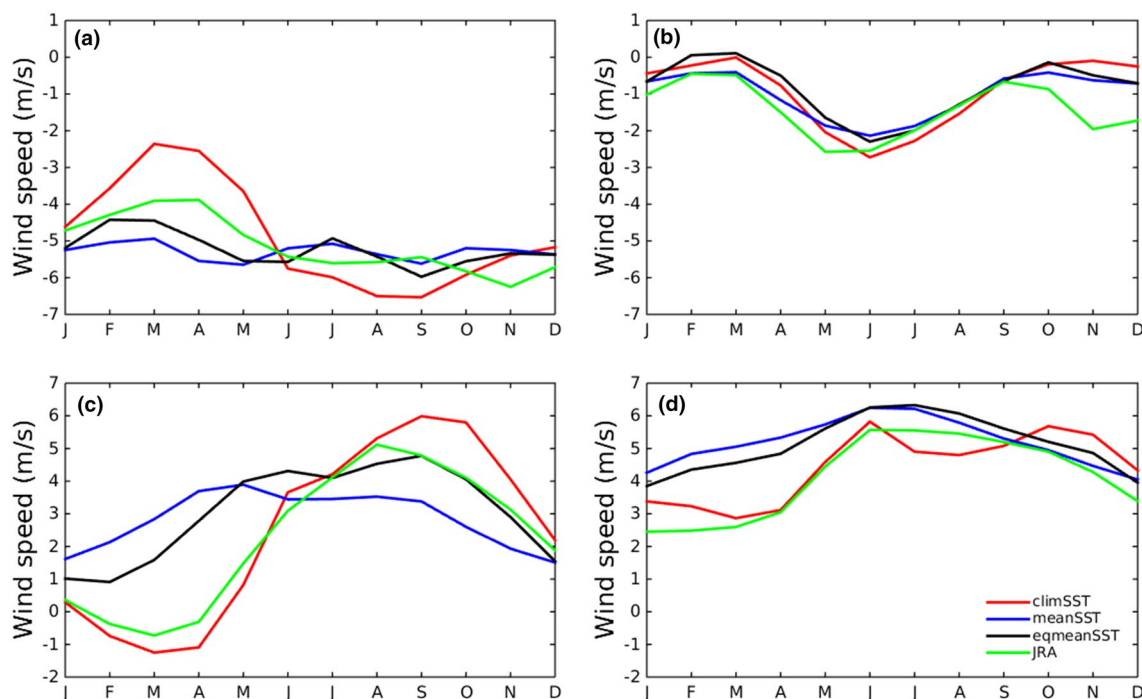

Fig. 4 Seasonal cycle of the surface winds in the WEA (4°S–4°N, 40°–20°W) (left panels) and EEA (4°S–4°N, 16°W–4°E) (right panels) regions for climSST (red), meanSST (blue) and eqmeanSST (black) runs and for JRA reanalysis (green). The panels (**a**) and (**b**) show the zonal winds, and (**c**) and (**d**) the meridional winds

seasonal cycle of EEA zonal winds. The semiannual cycle in zonal wind is poorly represented in all simulations, as they miss the strengthening of the zonal winds in October and November.

The impact of SST outside the equatorial Atlantic on the surface winds is estimated by comparing the meanSST and eqmeanSST runs (blue and black lines, Fig. 4). The EEA surface zonal winds have a similar seasonal evolution in EEA in both runs, with the largest difference during February to May. The annual cycle of meridional winds in the EEA is quite similar in both runs, while in the WEA the seasonal cycle is stronger in the eqmeanSST run. In summary, local SST have a large impact on the seasonal cycle of surface zonal and meridional winds in the WEA and on

meridional winds in the EEA, while remote SST have only a secondary role.

Our model (climSST run) captures the seasonal cycle of the precipitation in the west and eastern tropical Atlantic, but it shows some discrepancies to the observations: in the east and the west the maximum during the boreal summer monsoonal season occurs later and is displaced south (Fig. 5c, d), which is a common issue in other AGCMs (Mohino et al. 2011). The phasing of the precipitation in the WEA region is weaker and not well captured in the run with the SSTs set to their annual mean globally (meanSST run) (Fig. 5e); over the EEA the ITCZ is constrained to a narrow band north of the equator, and it does not migrate northward during boreal summer as in observations (Fig. 5f). Moreover, the

Fig. 5 Latitude-time precipitation Hovmoeller diagram for TRMM dataset (a, b), climSST (c, d), mean SST (e, f) and eqmeanSST (g, h) for the WEA (left panels) and EEA (right panels) regions. The monthly mean data has been longitudinally averaged along (35–15W) and (10W–10E) for WEA and EEA regions, respectively. Total precipitation is shown in blue shading. The differences between meanSST and climSST, and between eqmeanSST and climSST are highlighted in the panels e–f and g–h, respectively, with grey solid (dashed) line contours showing positive (negative) values
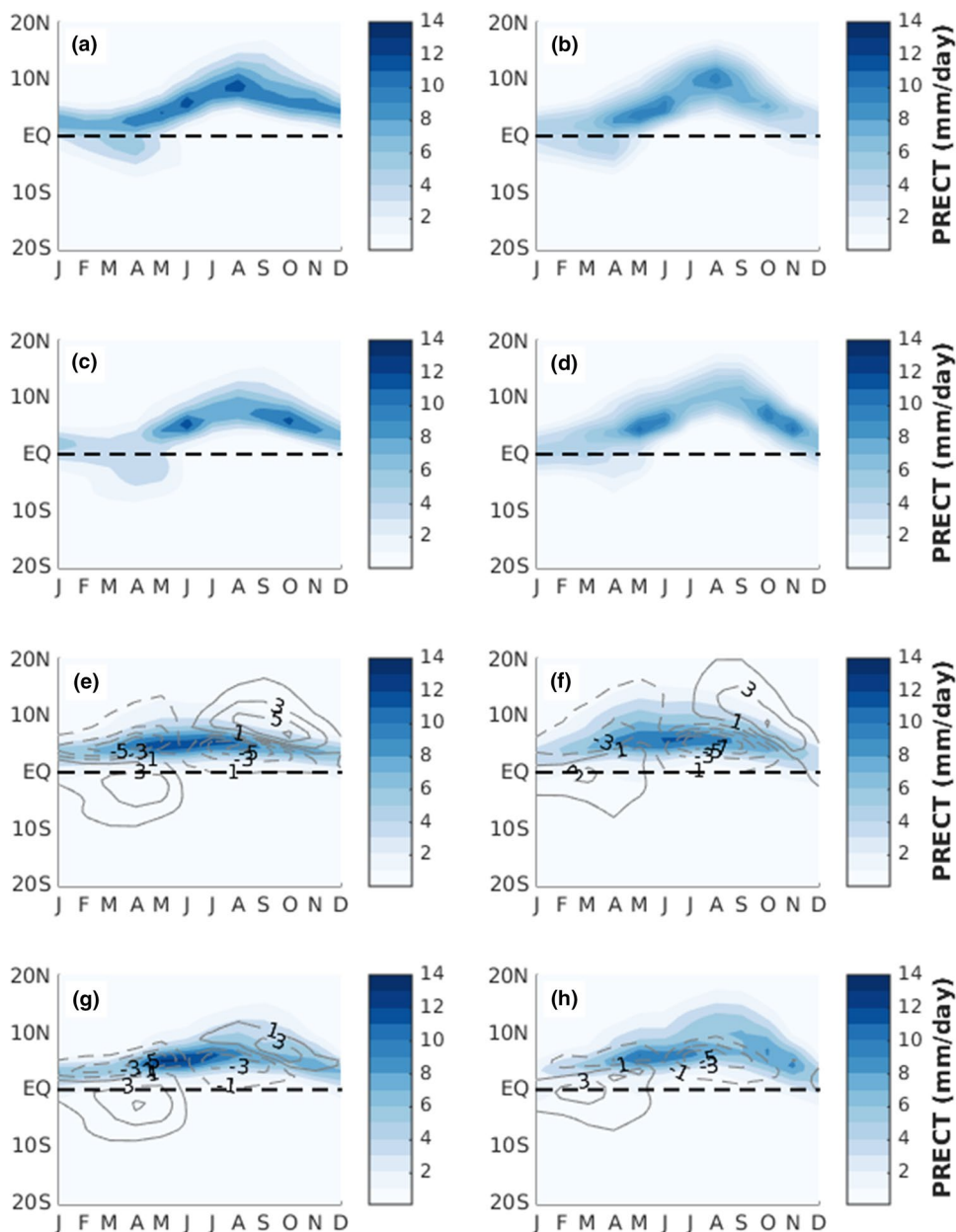
characteristic two maxima are not present in the meanSST run, but only one prolonged maximum in June-to-July instead, in agreement with the evolution of the meridional wind (Fig. 4d). The SST at seasonal timescales has a stronger impact on the precipitation patterns in the WEA comparing to that in EEA (Fig. 5e–h), where the latitudinal position of rain band still fluctuates even with annual mean global SST (meanSST) (Fig. 5e, f). The maximum in precipitation does not migrate but significant amount of precipitation (up to 6 mm/day) is present at 10°N (Fig. 5f). In the western equatorial Atlantic, the precipitation band is constrained to a much narrower band (4–8°N) for the same simulation without seasonality in global SSTs (Fig. 5e). Constraining only the equatorial Atlantic SST to its annual mean reduces the latitudinal extent of the seasonal migration of the ITCZ in both the eastern and western Atlantic (Fig. 5g, h).

The impact of equatorial Atlantic variations in SST is estimated by the differences between climSST and eqmeanSST experiments (Fig. 6). The precipitation difference is minimum in winter (DJF), coinciding with minimum SST difference (i.e., when the SST most resembles the annual mean). During the spring (MAM), the observed SST reaches its maximum so that SST in climSST is warmer than

in eqmeanSST, and this favours more rainfall over the equatorial Atlantic (Fig. 6b). In summer (JJA), the ACT is fully developed enhancing the northward displacement of the ITCZ over the Atlantic in climSST run (Fig. 6c). In SON the ACT is still distinguishable and the precipitation differences are similar to those in summer (Fig. 6d). The effects of the ACT on precipitation are mainly local and over the ocean, but remarkable differences in rainfall are still observed over land in northeast of Brazil in MAM, and West Africa during the JJA season. The development of the Atlantic cold tongue during boreal summer suppresses rainfall along the Gulf of Guinea coast, leading to a more developed West African Monsoon in climSST. Similar enhancement of regional monsoon circulation due to the cold SST can be seen in East Asian Monsoon system (e.g., Koseki et al. 2013).

4.2 Statistical quantification of the impact of the SST on the atmosphere at seasonal timescales

In this subsection, we present a statistical comparison of simulated atmospheric variables between climSST and eqmeanSST runs to quantify to what extent atmospheric
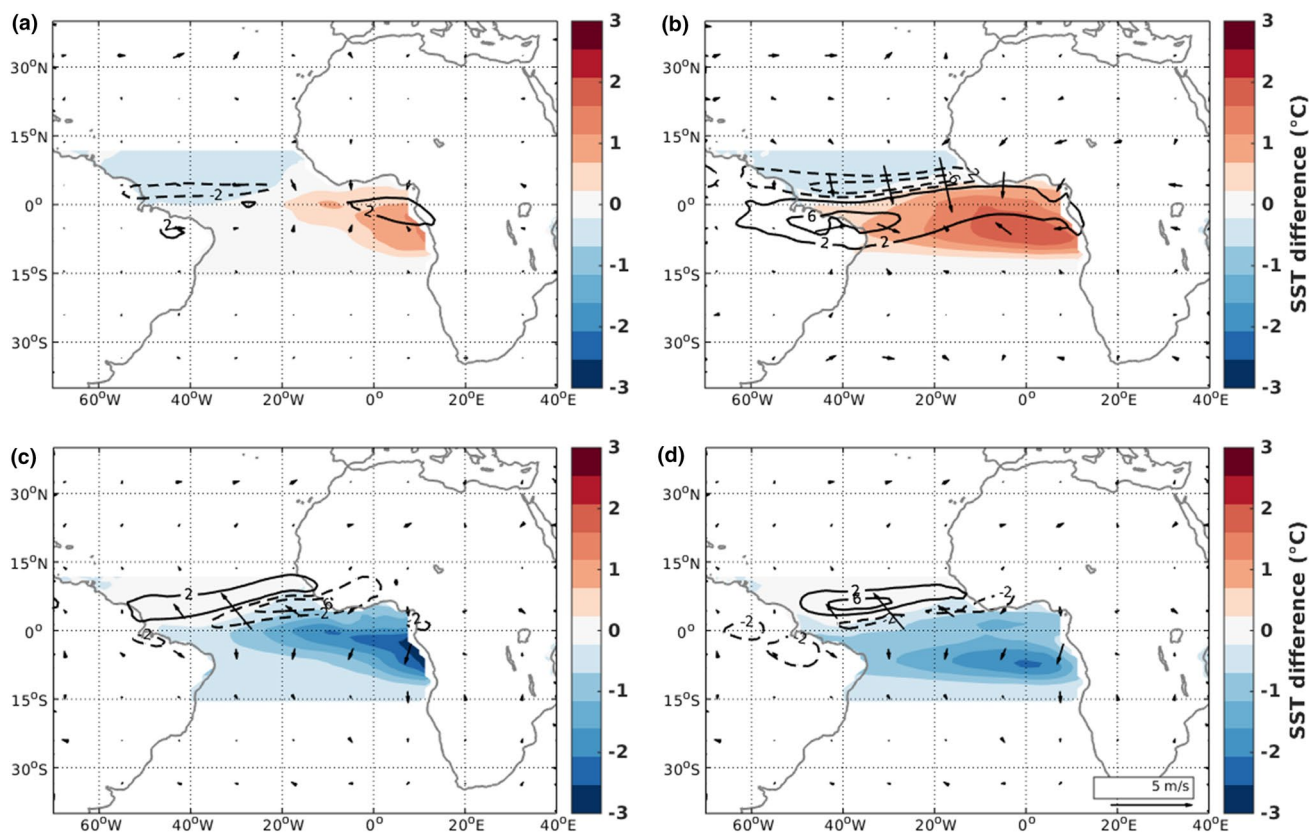

Fig. 6 Differences in rainfall (contours), surface winds (vectors) and SST (shading) between climSST and eqmeanSST runs by seasons. Negative (positive) differences in rainfall are represented with dashed (solid) lines. Negative and positive differences in SST are shown in blue and red, respectively. All the units are the same as in Fig. 1

seasonal variability is controlled by the seasonal cycle of the equatorial Atlantic SST. The MSE identifies the regions where there are larger differences between runs, i.e. where the equatorial SST is more relevant.

The decomposition of the MSE (see Eq 1 in the "Appendix") identifies the terms contributing most to increase the differences between the runs. The bias (Fig. 7d–f) is an indicator of the annual mean difference between the runs. Variances (Fig. 7g–l) contribute to the MSE when their magnitude is high and they differ between the two runs, and the covariance between them is low (Fig. 7m–o). In this analysis, the regions with high (low) covariance are those where the equatorial Atlantic SST has little (strong) influence on the atmosphere, and in this case the similar (differing) seasonal evolution in the two model runs does not (does) increase the MSE.

The bias and variance terms for precipitation are substantial and contribute to the MSE (Fig. 7d, g, j). The bias

in precipitation is consistent with the strongly reduced seasonality in the latitudinal position of the ITCZ in the eqmeanSST (and meanSST) run (Fig. 5g, h), and this is also evident in the lower variance in the eqmeanSST run (Fig. 7j) with respect to the climSST run (Fig. 7g). There is a high positive covariance between climSST and eqmeanSST runs in the ITCZ region north of the equator in the western Atlantic, and in the far eastern equatorial Atlantic, and over continental regions (Fig. 7m). The covariance is low for precipitation over the western and central equatorial Atlantic and this leads to a high MSE in these regions.

The bias is relatively low for zonal and meridional surface winds and the variance terms mostly explain the MSE. Compared to climSST, the variance in zonal wind in eqmeanSST is less in the western equatorial Atlantic (Fig. 7h, k), and the variance in meridional wind is less in both the western and northwestern equatorial Atlantic (Fig. 7i, l). The covariance between eqmeanSST and climSST runs is also
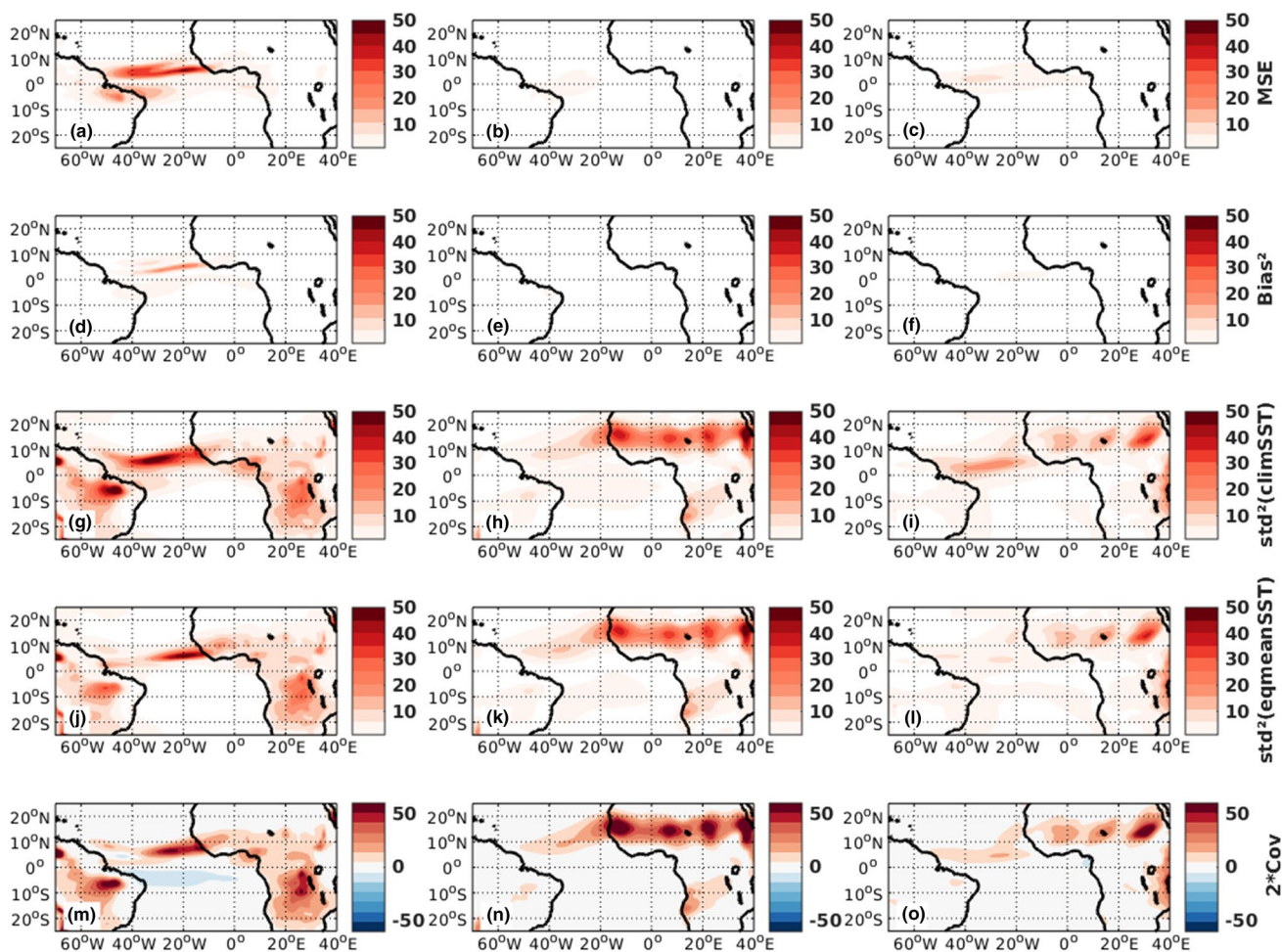

Fig. 7 Terms contributing to the mean square error between climSST and eqmeanSST runs of precipitation (left column), zonal (center column) and meridional (right column) winds. Total MSE (first row), bias (second row), standard deviation of the climSST (third row) and eqmeanSST (fourth row) runs, and covariance (fifth row) are shown. The units of the precipitation and the surface winds are mm^2 and m^2/s^2, respectively

low for surface wind in these regions (Fig. 7n, o). The MSE in the eastern equatorial Atlantic is mostly related to low covariance.

In our framework, the squared correlation maps for simulated precipitation and surface winds between climSST and meanSST (eqmeanSST) runs are a measure of the variance explained in these quantities in the absence of seasonal variability in global (equatorial Atlantic) SST (Fig. 8). A low (high) squared-correlation indicates that the impact of the seasonal variability of the SST is strong (weak). The seasonal cycle of the global SST can explain a high amount of the variance of the precipitation over the tropical Atlantic Ocean, with the exception of a narrow equatorial band in the western and easternmost sides of the basin (Fig. 8a). A high amount of the variance of terrestrial precipitation surrounding the tropical Atlantic basin can be explained without the annual cycle in global SST: 50–70% in the central/north Sahel and 80–100% in subtropical South America and Southern Africa. Thus, the monsoonal flow, which is generated by the land–ocean heat contrast and mainly controlled by the land surface temperature, seems to be the main driver of the precipitation in the Sahel region. However, our results suggest that there is also a smaller, but remarkable impact of SST on the rainfall over that region (Fig. 8a). Most of the seasonal cycle of the zonal wind in central equatorial Atlantic, Sahel and Amazon can be explained without the seasonal changes in the global SST (Fig. 8b). This is not the case in the western equatorial Atlantic, far eastern equatorial Atlantic, and northeast of Brazil (Hastenrath 2012), where the SST is known to play a key role in the determination of the seasonal cycle of the atmosphere. The SST seasonal cycle is crucial to induce the seasonal cycle in meridional wind along the equatorial Atlantic basin (Fig. 8c). The SST is also relevant for the determination of the winds along

the *WAM generation oceanic region* as defined by Gallego et al. (2015).

The equatorial SST mostly affects the seasonal cycle of the atmosphere locally (Fig. 8d–f). Equatorial Atlantic SST variability explains most of the precipitation seasonal cycle over the equatorial Atlantic and has relevant impacts on precipitation for coastal areas of both South America and West Africa (Fig. 8d). In particular, around 40–60% of the precipitation cannot be explained in the absence of equatorial SST variability in the coastal Sahel. In central and north Sahel, the SST outside the equatorial Atlantic, explain up to 60% of the precipitation variance (from comparison between Fig. 8a, d). In the northeastern Brazil the precipitation is highly dependent on the equatorial Atlantic SST, with more than 80% explained variance from 10S to 10N along the coastal regions (Fig. 8d). The zonal wind is also highly influenced by the equatorial Atlantic SST in the WEA and in coastal EEA, but it seems independent of SST variability in the central equatorial Atlantic (Fig. 8e). Equatorial SST variability explains most of the variance of the meridional wind over the Gulf of Guinea (Fig. 8f). The comparison between the set of Fig. 8a–c, d–f indicates that SST outside the equatorial Atlantic have a remote impact in the equatorial band, especially in the surface winds at WEA region. In the particular case of the zonal winds, the comparison between Fig. 8b, e shows that the variability of the off-equatorial SSTs explain more variance in zonal winds in the WEA than equatorial SSTs. [Note that blue (red) indicates variance (not) explained by SSTs]. It also shows that SST variations outside the equatorial Atlantic are more important for the seasonal cycle of Sahel rainfall (Fig. 8a, d).

This analysis indicates that equatorial Atlantic SST variability is the main driver of the seasonal cycle in precipitation
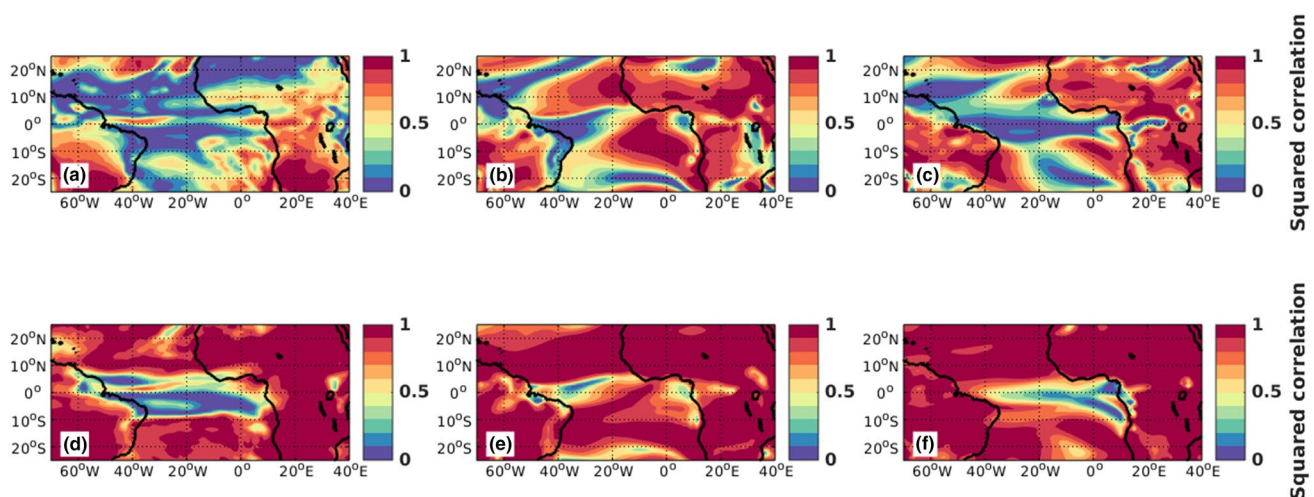

Fig. 8 Squared correlation between climSST and meanSST runs (top row) and between climSST and eqmeanSST runs (bottom row), for the precipitation (left), zonal (center) and meridional winds (right)

and surface winds in the western equatorial Atlantic, and it drives a substantial portion of seasonal cycle in precipitation and meridional winds over the eastern equatorial Atlantic.

4.3 Co-variability of the tropical Atlantic ocean-atmosphere-land coupled system at seasonal timescales

As shown in the previous subsection, low covariance is the main cause of the MSE between the control (climSST) and sensitivity (meanSST and eqmeanSST) runs in terms of the annual cycle of atmospheric quantities. A further analysis of the co-variability modes between ocean, land and atmosphere using MCA (see "Appendix") is performed to understand more deeply how the different components of the ocean-atmosphere-land system covary with each other, and to identify the role of the SST in the annual cycle. We only show the 1st covariability mode because in every case it explains by far the most of the squared covariance in all MCA cases we perform (97–99%); this confirms the dominance of the seasonal cycle in the tropics. We perform MCA for three different cases: climSST-meanSST, meanSST and climSST-eqmeanSST (Sect. 3.2). In climSST-meanSST case

we investigate the coupled modes between atmosphere and SST over the tropical Atlantic domain while in climSST-eqmeanSST we investigate coupled variability only over the equatorial Atlantic domain. In the meanSST case, we analyze the coupled modes of the LST and atmosphere over the tropical Atlantic.

We consider the first MCA case on coupled variability between the ocean and atmosphere in the whole tropical Atlantic (climSST-meanSST). The homogeneous SST regression map shows a marked interhemispheric temperature gradient associated with the seasonal variations in insolation, with out-of-phase anomalies in the southern and northern hemispheres. However, the ocean dynamical processes contribute to several features in the SST maps not directly related to insolation: strong Senegal-Mauritanian and Angola-Benguela coastal upwellings, and the characteristic development of the cold tongue in the Gulf of Guinea during boreal summer (Fig. 9a). The precipitation and surface winds in the tropical band exhibit a prominent seasonal evolution (Fig. 9b) that is synchronized with the SST thermal forcing, with maximum anomalies in late boreal summer when the ITCZ is displaced to the north (Fig. 9c). The seasonal evolution of the ITCZ (in the
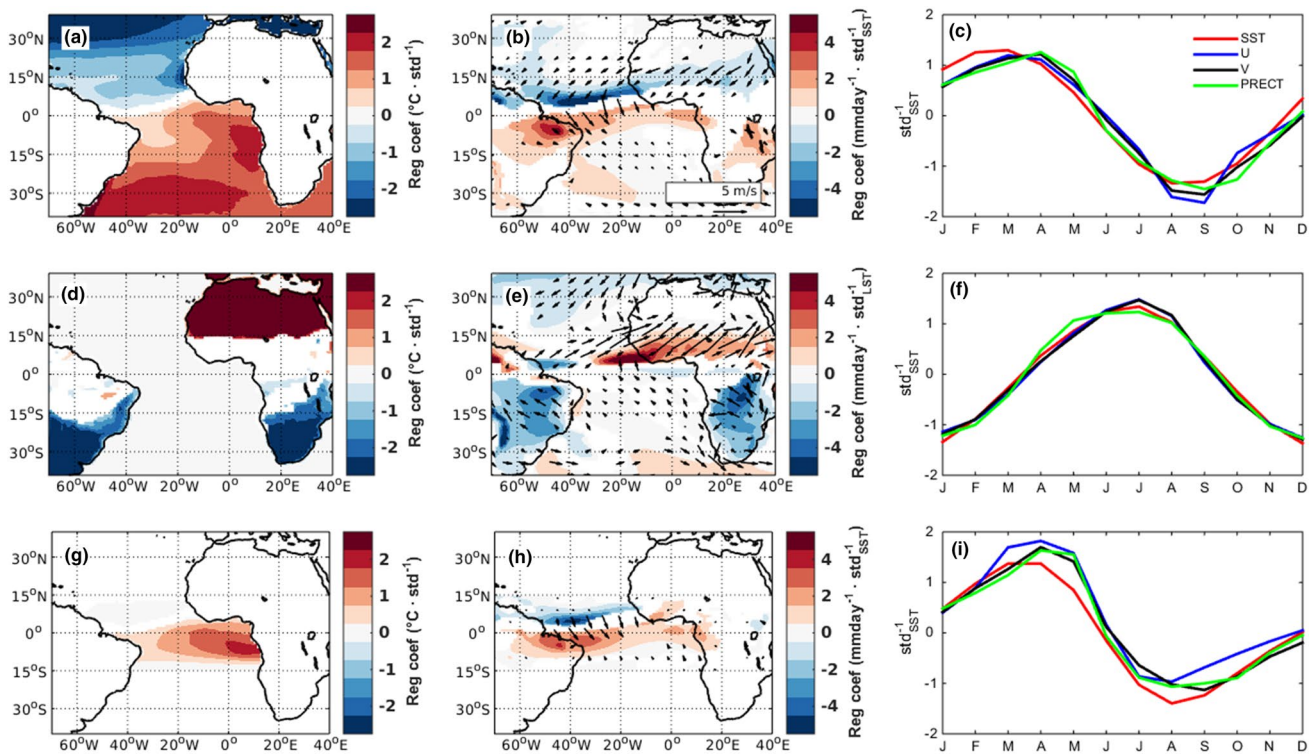

Fig. 9 (Top row) Spatial patterns of the first mode of the MCA between SST and atmospheric fields for climSST-meanSST case. SST homogeneous map (left panel), SST-(PRECT, U, V) heterogeneous map (center panel) and expansion coefficients (right panel) of the coupled fields. In the heterogeneous map, surface winds are represented with vectors and SST with shaded contours. All units

are standarized to the predictor variable units. Only 95% significant anomalies are shown. The first mode accounts for more than 96% of the squared cross-covariance for every pair of variables. (Central row) Same as top row but for meanSST case with LST as the predictor variable instead of SST. (Bottom row) Same as top row but for climSST-eqmeanSST case

MCA coupled SST-atmosphere mode) is evident over the entire equatorial Atlantic Ocean. West African precipitation does not depend much on the SST, while northeastern Brazil does (Fig. 9b).

The dominant MCA mode of LST versus atmospheric variables in the meanSST case highlights the influence on the atmosphere of the seasonal variability of the LST, which is mainly controlled by that of the insolation. The homogeneous LST map (Fig. 9d) shows an interhemispheric temperature gradient analogous to that in the SST in the previous case. The maximum interhemispheric differences in LST coincide with the seasonal march of the sun (Fig. 9f). The comparison among the expansion coefficients of climSST-meanSST and meanSST cases reveals that the SSTs influence the timing of the precipitation. The coefficient of expansion for the SST MCA mode has the precipitation peak in August–September (Fig. 9c), coinciding with the fully developed cold tongue, while the LST MCA mode has the precipitation peak in July (Fig. 9f). Ocean thermodynamical and dynamical processes likely cause the maximum interhemispheric differences in SST to lag that in insolation by 1–2 months. The coupled heterogeneous regression map shows that LST is highly related to the Sahelian precipitation over the western Africa and with the associated southwesterly winds during boreal summer (see Fig. 9e). A clear monsoonal pattern is evident with strong large-scale winds blowing from the ocean towards the land from April to September transporting moisture and triggering the precipitation over land in Sahel. In the equatorial band we can easily distinguish two rainfall regimes; oceanic and continental precipitation, mainly controlled by ocean (SST; Fig. 9b) and land (LST; Fig. 9e) seasonal cycle variability, respectively (Gu and Adler 2004).

The ocean–atmosphere coupled mode when we only consider the equatorial SST variability (climSST-eqmeanSST case) closely resembles that of the case when we consider the global SSTs impact (climSST-meanSST case), but appears to be more localized at the equator (bottom row in Fig. 9). The equatorial SST is the main driver of the precipitation and low-level winds over the equatorial Atlantic Ocean (Fig. 9g, h). Over land, it exhibits a remarkable impact over the northeast of Brazil, where SST triggers intense precipitation during the boreal spring season (Fig. 9h, i); there is also a limited impact on coastal West African precipitation. The comparison of equatorial (bottom row in Fig. 9) and tropical (top row in Fig. 9) Atlantic SST MCA modes indicates that off-equatorial SST anomalies play a more important role in the northward migration of the ITCZ over the West African continent. Nevertheless, the equatorial cold tongue appears to play an important role in the sudden onset of WAM in boreal spring (Fig. 9i, and also Figs. 4, 5).

Our results show that the precipitation and low-level wind circulation over the Atlantic Ocean and equatorial Brazil rainfall are driven by the seasonal cycle of the equatorial Atlantic SST. LST and off-equatorial SST mostly determine the northward migration of the ITCZ in the WAM region, but equatorial SST contributes to the onset of the WAM.

4.4 Dynamics driving the low-level wind convergence in the equatorial Atlantic at seasonal timescales

In this section we explain the dynamical connection between SST and surface winds in the equatorial Atlantic. Takatama et al. (2012) performed a diagnosis of the wind convergence budget by decomposing it into three major contributions: the so-called pressure adjustment mechanism (Lindzen and Nigam 1987), the downward momentum mixing mechanism (Wallace et al. 1989; Chelton et al. 2001; Zermeño-Diaz and Zhang 2013) and a term related with horizontal advection. We follow their approach using our AGCM output to evaluate the relevance of the pressure adjustment mechanism in driving the wind surface convergence over the equatorial Atlantic. In this mechanism, the surface wind convergence is linearly proportional to the Laplacian of the SLP, and a weaker opposite relation is expected between SLP and SST Laplacians (see "Appendix").

Figure 10 shows the spatial distribution of the wind convergence, SLP Laplacian and sign-reversed SST Laplacian, computed from the differences between climSST and eqmeanSST for each horizontal component in July (when the wind convergence is stronger). Note that this analysis excludes seasonal variations in winds not related to equatorial Atlantic SST. The meridional components of the sign-reversed SST Laplacian and SLP Laplacian are much larger than the zonal ones and they can explain most of the variance of the total wind convergence. They match quite well over the regions where the meridional SLP Laplacians and convergence are strong, in particular, in the oceanic ITCZ region. A weaker but remarkable relationship is also present between meridional component of the SLP Laplacian and sign-reversed SST Laplacian in that region.

Focusing on the equatorial band, we see a stronger relation over the EEA than over the WEA in July (Fig. 10). The relationship between SLP Laplacian and wind convergence remains strong (correlation ~ 0.64) in EEA region when considering all calendar months (Fig. 11a), and it is weak in the WEA (not shown). The weaker positive correlation between SLP and sign-reversed SST Laplacians remains in the EEA when considering all calendar months (Fig. 11b). Thus, the pressure adjustment mechanism appears to hold in the east of the basin.

The spatial variations in the relation among the different terms in the pressure adjustment mechanism are investigated across the equatorial Atlantic, by using 1.25° longitude and 8° latitude (4S–4N) zonally sliding window correlations and
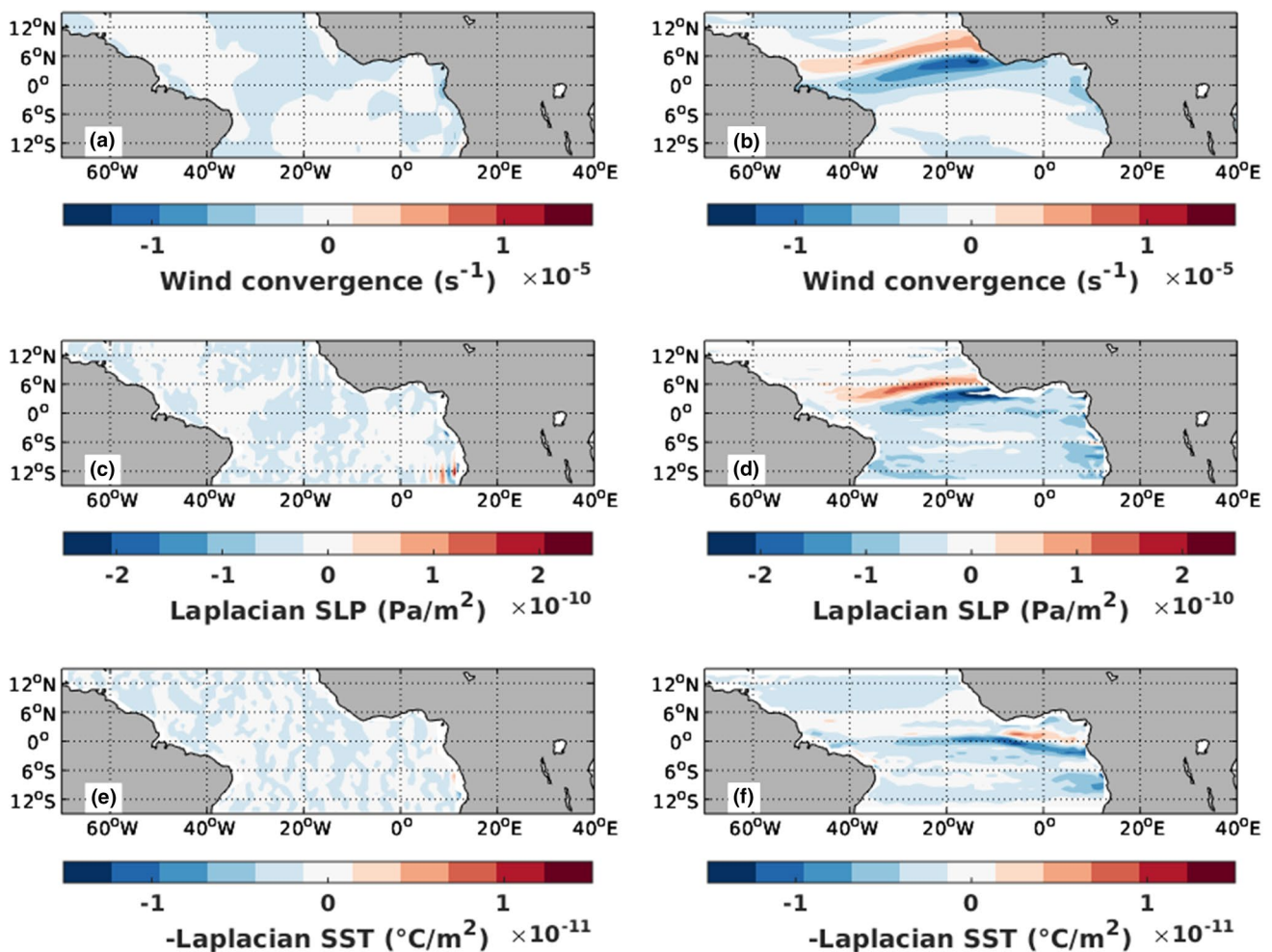
Fig. 10 Surface wind convergence (top row), SLP Laplacian (central row) and sign-reversed SST Laplacian (bottom row) over equatorial Atlantic basin for the difference between climSST and eqmeanSST runs in July. Zonal and meridional components are shown in left and right columns, respectively. Red and blue regions correspond to positive and negative values of the Laplacian and to convergence and divergence zones, respectively

considering all calendar months (Fig. 12). The validity of the mechanism extends from the eastern equatorial Atlantic to the center of the basin (around 20W) with correlations between SLP Laplacian and wind convergence exceeding 0.7, and correlations between SLP and SST Laplacian around 0.3 (Fig. 12a, d). In the far western Atlantic the correlations are in both cases weak and even negative. The relation is mainly determined by the meridional component of wind convergence, SLP Laplacian, and sign-reversed SST Laplacian (Fig. 12c, f). This result is consistent with seasonal variations in zonal winds in the central equatorial Atlantic not being driven by seasonal variations in SST in our experiments.

The greater importance of the Lindzen and Nigam (LN hereafter) model framework in the east is also consistent with the prevailing easterly winds that induce a shallow thermocline in the east, favouring dynamically driven

SST variations and air–sea interactions. Here the coupling between ocean and atmosphere is determinant for the evolution of the low-level tropospheric wind field and convergence. On the other hand, in the western Atlantic with a deeper thermocline, the air–sea interactions play a secondary role in the wind convergence, which cannot be explained by the pressure adjustment mechanism.

The zonal components of SLP Laplacian and wind convergence do not follow the LN model in the equatorial Atlantic. Even if the SST is strongly correlated with the SLP, the relationship between SLP Laplacian and wind convergence (Fig. 12b) is less than expected following the LN model (see Eqs. 12 and 13 in the Appendix). This implies that the zonal wind convergence in equatorial Atlantic is driven by other mechanims. Richter et al. (2014) found no clear relationship between surface zonal winds and sea level pressure and showed that the
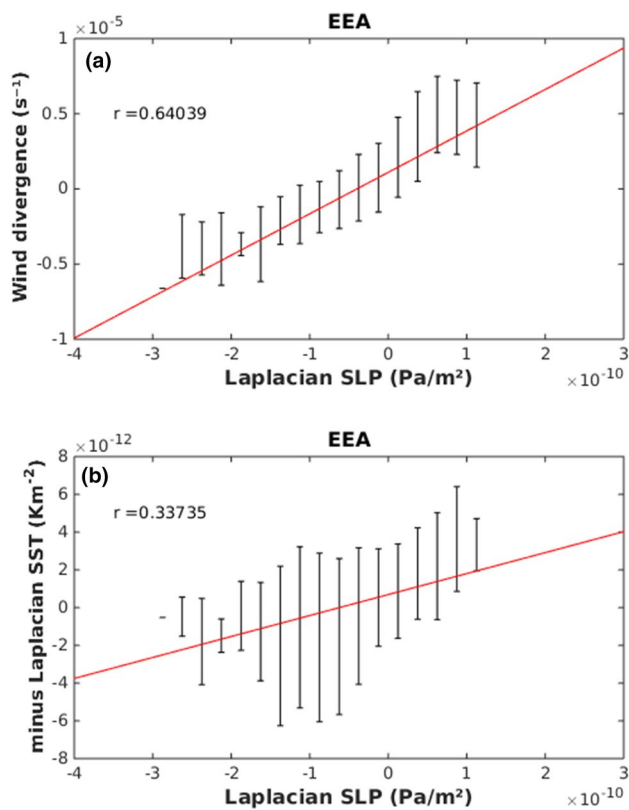
Fig. 11 **a** Relationship between the SLP Laplacian and wind convergence and **b** SLP Laplacian and sign-reversed SST Laplacian for the difference between climSST and eqmeanSST runs for EEA and every calendar month

downward momentum mixing mechanism is the main driver of the zonal winds during the MAM season in the WEA. Our results are consistent with this mechanism being a main contributor to the zonal wind convergence budget along the whole year since the correlation between SLP Laplacian and wind convergence is weak when considering all months (Fig. 12b).

In summary, in the central and eastern equatorial Atlantic we identify the LN mechanism as the main dynamical driver of the surface meridional winds; this is in agreement with the remarkable influence of equatorial SST variability on the meridional winds in this region. In the case of the zonal winds, which are insensitive to seasonal changes in SST, the LN model does not provide an explanation for the seasonal variations in zonal winds in the region. In the western Atlantic, we find no indications of LN model playing a dominant role in driving any of the wind components. The strong sensitivity of the surface winds to changes in the SST field indicates that another mechanism involving SST fronts is driving the wind convergence in the western equatorial Atlantic.

5 Summary and discussion

We have investigated the impact of the ocean on the atmosphere at seasonal timescales in the equatorial Atlantic region. We have performed a set of AGCM experiments especially designed to elucidate the role of the SST in atmosphere-ocean-land interactions in the seasonal cycle of the equatorial Atlantic. Our model results suggest a dominant influence of the seasonal variability of equatorial Atlantic SST on the precipitation over the equatorial Atlantic Ocean and over land in equatorial South America and in the Gulf of Guinea. Equatorial Atlantic SST do not have a strong influence on the WAM, as the seasonal cycle of precipitation over West Africa is reasonably represented in our simulations with annual mean equatorial SST. Although LST and off-equatorial SST play a more important role for the WAM, equatorial SST variations are critical for the abrupt shift in the meridional winds over the eastern equatorial Atlantic that are characteristic of the onset of the WAM. The meridional winds in the eastern equatorial Atlantic are strongly coupled with seasonal variations in SST, in stark contrast with the seasonal variations of zonal winds over the central equatorial Atlantic that show little dependence on the seasonal cycle of SST. On the other hand, the meridional and zonal winds over the western equatorial Atlantic are both strongly related to seasonal variations in equatorial Atlantic SST.

Equatorial Atlantic SST also explains a significant fraction of the seasonal variability of the rainfall over northeast Brazil (up to 80%) and coastal regions in the Gulf of Guinea (up to 50%), and global SST variations can explain large fractions of rainfall variability over continental tropical South America and Africa. The MCA coupled modes show that the precipitation and low-level wind circulation over the Atlantic Ocean and equatorial Brazil rainfall are driven by the seasonal cycle of the equatorial Atlantic SST. The seasonal evolution of LST and SST away from the equator mostly determine the northward migration of the ITCZ in the WAM region, but equatorial SST contributes to the sudden onset of the WAM in boreal spring. The main coupled MCA variability modes show the coexistence of two rainfall regimes (Gu and Adler 2004) in the tropical Atlantic, oceanic and continental rainfall, that are controlled by the seasonality of SST and LST, respectively.

In the eastern and central equatorial Atlantic, the atmospheric internal variability and land–ocean–atmosphere interactions are the major drivers of the low-level flow. The LN mechanism can explain the contribution of the ocean–atmosphere interactions to the low-level meridional winds. Strong meridional SST gradients modify the surface pressure field forcing strong meridional SLP gradients, which in turn drive the surface wind convergence.
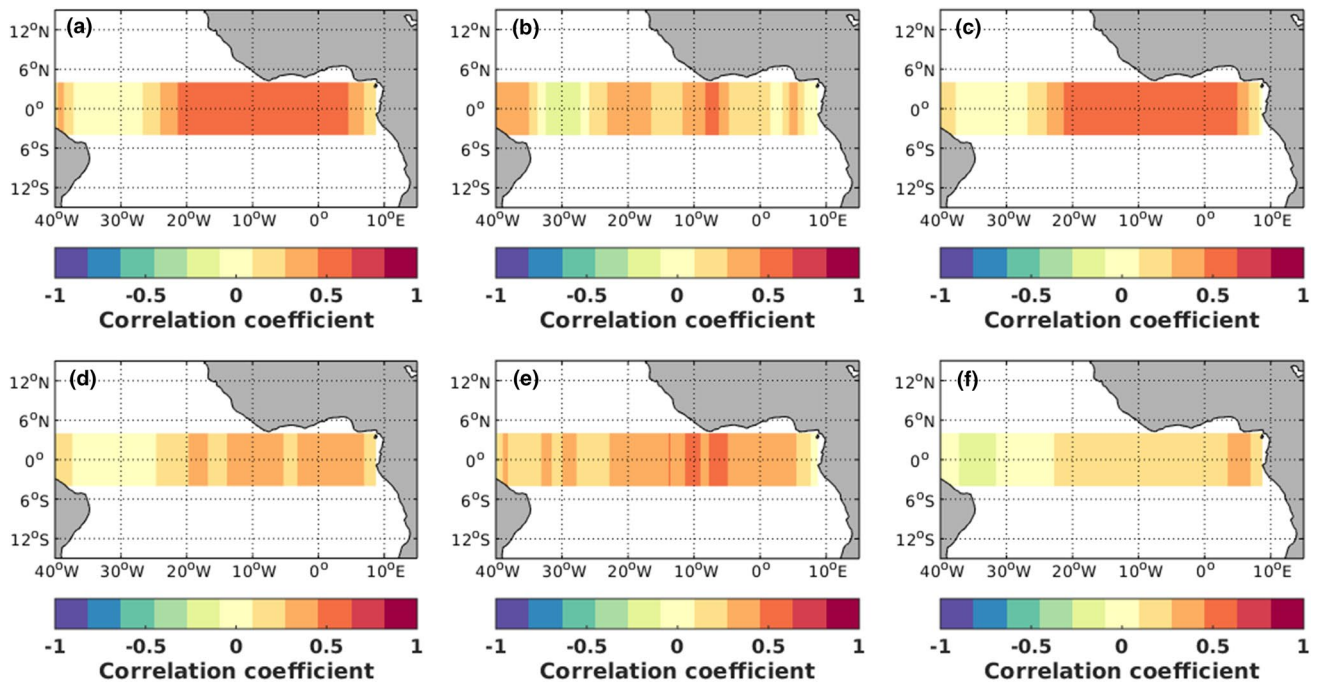
Fig. 12 Correlation maps of the SLP Laplacian and wind convergence (top row) and SLP Laplacian and sign-reversed SST Laplacian (bottom row) for sliding lat-lon boxes covering the equatorial Atlantic (4°S–4°N) basin. The left column shows the total contribution, and the central and right column show the zonal and meridional components, respectively. The sliding boxes are taken every 1.25° in longitude for the fixed latitude band (4°S–4°N). The correlations are calculated taking into account every calendar month

As suggested by previous studies, the zonal and meridional winds along the equator might be driven by different mechanisms. The meridional winds in the eastern equatorial Atlantic are well explained by the LN model (Richter et al. 2014, Diakhaté et al. 2018). In the western equatorial Atlantic, the LN model appears to only explain meridional wind variations at the northern and southern flanks of the ITCZ (Diakhaté et al. 2018). The zonal wind variations cannot be explained by the LN model but are likely related to entrainment and vertical mixing of zonal winds, meridional advection of zonal winds, and the large-scale response to elevated diabatic heating (Gill 1980, Zermeño-Diaz and Zhang 2013, OX04, Richter et al. 2014, Diakhaté et al. 2018). A complete computation of the zonal momentum budget would give a deeper insight into the mechanisms controlling the zonal momentum budget, but is beyond the scope of this study.

In terms of the two contrasting views on the role of SST in the eastern tropical Atlantic seasonal cycle, our results are in greater agreement with OX04 as they indicate that ACT impacts the seasonal cycle of meridional winds in the eastern equatorial Atlantic, rather than LP97 who identify little impact of equatorial Atlantic SST. However, while OX04 show that the development of the ACT has a remarkable impact on the rainfall over West Africa, we find only a muted impact more in line with Druyan and Fulakeza

(2015). A likely reason for the difference could be the different experimental design. OX04 compare simulations where the seasonal cycle of equatorial Atlantic SST is set to a constant value from April onwards (i.e., when SST in the east is warmest) to simulations with a normal development of the ACT. While in our experiments we compare annual mean equatorial SST with the normal SST seasonal cycle. Thus, their equatorial SST anomalies during JJAS are approximately twice as large as ours. The larger land–ocean temperature contrast in their experiments likely enhances the precipitation response over West African continent. Therefore, the existence of previous warm SST in April appears a dominant factor for a further penetration of the ITCZ into the continent. A second reason for discrepancies could be the sensitivity to the model formulation. In particular, Druyan and Fulakeza (2015) apply a very similar SST forcing to OX04, but in a regional model configuration with limited ensemble size, and find the development of the ACT has little impact on the timing and northward migration of the monsoon. Differences between our results and those of LP97 in terms of the meridional winds also suggest a degree of model sensitivity, which might reflect differences in the modelling capabilities between several model generations. In agreement with both LP97 and OX04 model experiments, we find that the seasonal cycle of zonal winds over the eastern equatorial Atlantic is not strongly influenced

by equatorial SST. However, OX04 argue based on budget analysis that the ACT does also influence the seasonal cycle of zonal winds over the equatorial Atlantic.

In terms of western equatorial Atlantic, our results agree with both LP97 and OX04 in showing that equatorial SST strongly influences the atmospheric seasonal cycle. Our finding that equatorial SST patterns strongly determine the seasonality of the winds in the western equatorial Atlantic is consistent with the Bjerknes positive feedback. In this mechanism, interannual variability in eastern Atlantic SST explains a large amount of the zonal wind variability over the western equatorial Atlantic, but explains little variability over eastern equatorial Atlantic (Keenlyside and Latif 2007). Thus, our results are consistent with the Bjerknes feedback playing a role in the equatorial Atlantic also at seasonal timescales. Note, as discussed above, that the impact of SST on zonal winds over the western equatorial Atlantic cannot be explained by the LN mechanisms; further research is needed to understand the SST impact on zonal winds in this region.

The Bjerknes feedback is one of the main mechanisms at play for the determination of the zonal gradients of SST and their relationship with zonal wind field but cannot explain the meridional SST pattern. Our finding that equatorial SST seasonal variations largely determine the pattern of the meridional winds throughout the entire equatorial Atlantic basin indicates that there must be another mechanism at play. Previous studies (Saravanan and Chang 2004; Chiang and Vimont 2004) have shown that the so-called meridional SST mode is largely determined by the wind-evaporation-SST (WES) feedback (Xie 1999; Saravanan and Chang 1999). Amaya et al. (2017) found that the WES feedback is the main contributor in driving the interhemispheric SST gradients at interannual to decadal timescales in the tropical Atlantic. In our modelling framework we found that WES-like feedback might play a role in the western equatorial Atlantic. In particular during all seasons of the year the latent heat flux anomaly in the WEA tends to drive the SST changes rather than damp them (not shown). In this region, the wind speed anomalies appear to be an important driver of the latent heat flux anomalies consistent with the WES mechanism. In EEA the pattern of latent heat flux anomalies damps the SST anomaly (that is, the ocean drives the heat flux anomaly). Further investigation on how the ocean responds to the wind field is needed to evaluate the relevance of the WES-like feedback in the equatorial Atlantic at seasonal timescales.

We showed evidences of the impact of the SST variability on surface meridional winds in the eastern equatorial Atlantic and proposed a dynamical mechanism explaining most of its variability, but surprisingly the seasonal cycle in SST does not seem to impact zonal winds in the central equatorial Atlantic. We hypothesize that the annual variability of the zonal surface winds in the central equatorial Atlantic

is related to the extratropical interhemispheric differential heating that controls the large-scale Hadley Circulation. This is supported by the boreal winter to summer difference of the surface winds at the equator, the sea-level pressure in the whole south and equatorial Atlantic sector (50°S–20°N), and the pressure-meridional cross section of the winds in our experiments (Fig. 13). The comparison between climSST and eqmeanSST simulations shows little difference in the three-dimensional circulation, in particular, the southerly wind difference between JJA and DJF at the lower troposphere, indicates that the Hadley Circulation is identical in both experiments (Fig. 13b, d). Thus, the contributions from the Hadley Circulation to the equatorial trade winds are almost unchanged between the two experiments.

The mismatch between the semiannual cycle of the insolation and the strong annual cycle in SST in the eastern equatorial Atlantic remains an open question that cannot be addressed by atmospheric model experiments. In particular, it is well known the western part of the equatorial Atlantic is dominated by a local response to the annual wind forcing, while the central and eastern Atlantic have a relatively strong semiannual cycle due to ocean adjustment processes (Philander and Pacanowski 1986); these are resonantly excited by a weak semiannual cycle in surface winds at the equator (Ding et al. 2009). Our results indicate that the strength of the coupling between ocean and atmosphere might play a decisive role in the determination of the seasonal cycle in the equatorial Atlantic, with an annual (semiannual) cycle in the west (east) where the ocean–atmosphere interactions are stronger (weaker). However, other reasons might explain why a semi-annual cycle in ocean dyanmics does not lead to semi-annual cycle in SST in the eastern equatorial Atlantic.

In summary, our study shows that the seasonality of equatorial SST is important for the seasonal cycle of precipitation and meridional winds across the equatorial Atlantic, and of zonal winds in the western equatorial Atlantic, and that seasonal variations in zonal winds over the eastern equatorial Atlantic are likely determined by large-scale interhemispheric differential heating. Given the importance of zonal winds in driving the seasonal cycle of equatorial Atlantic SST, further investigation on the potential feedback of zonal winds on SST is needed to completely understand the role of the coupling between the ocean and the atmosphere at seasonal timescales in the equatorial Atlantic. Coordinated model experiments including momentum budget analysis would be very beneficial to understand the sensitivity of the results to model formulation and the impact of model biases. This is a priority given the large tropical Atlantic climatological biases that exist in the state-of-the-art models.
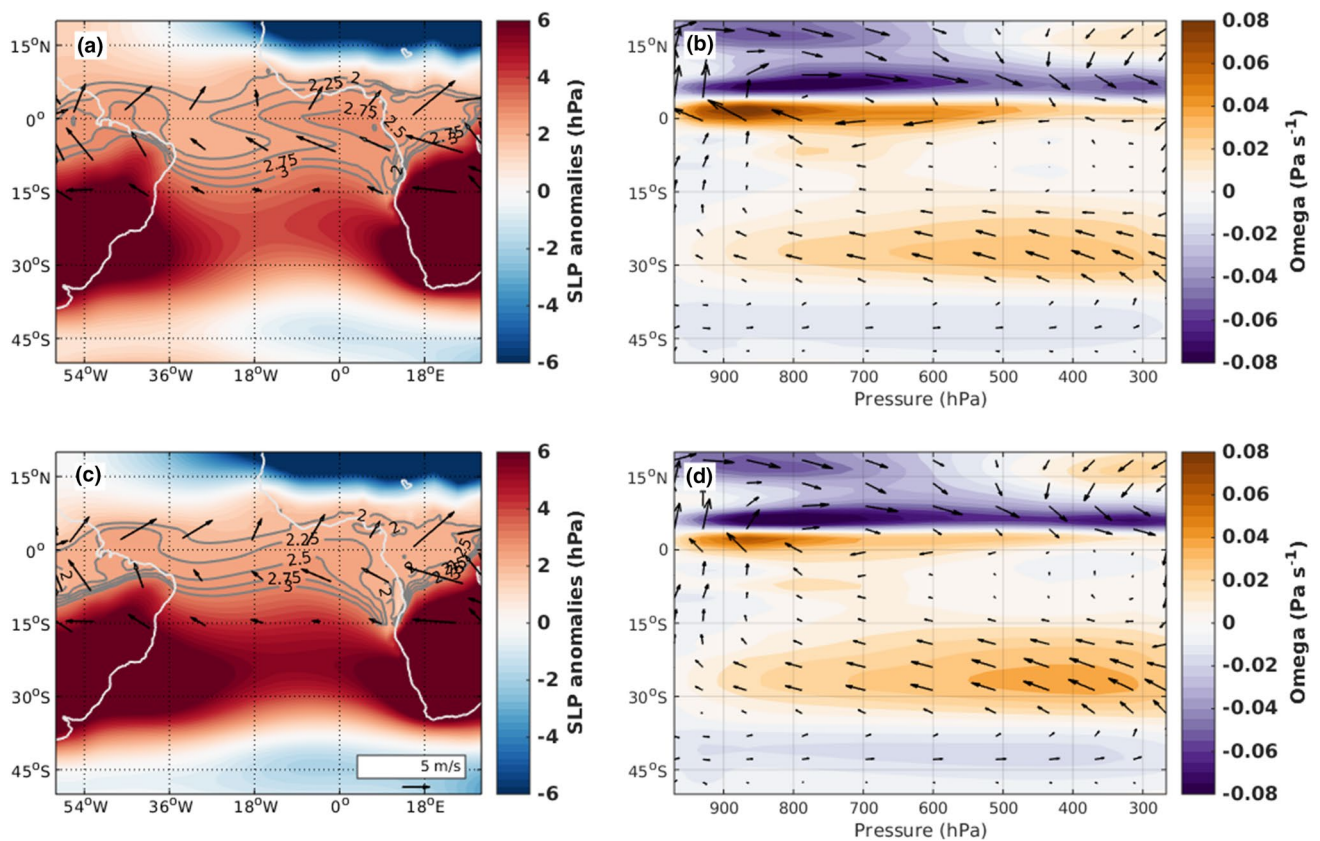
Fig. 13 Sea-level pressure anomalies of the winter to summer difference (JJA-DJF) for **a** climSST and **c** eqmeanSST simulations. The pressure contours at the equator are highlighted in grey contours. Surface winds are shown as vectors and shading shows positive (negative) sea-level pressure anomalies from the annual cycle in red (blue). The right panels show the pressure-meridional cross-section of the large-scale circulation for **b** climSST and **d** eqmeanSST simulations.

Shading shows positive (negative) vertical velocity in orange (purple). Meridional-vertical winds are shown as vectors. The right panels have been inverted showing latitude in the y-axis and pressure in the x-axis so they match the latitude in the left panels, in order to facilitate the identification of the 3-dimensional large-scale circulation in the tropical Atlantic

Appendix

Model-to-model verification

We analyze how eqmeanSST run values differ from climSST run, which will give us a hint of the impact on the atmosphere of the tropical and equatorial oceanic SST variability, respectively.

According to the Eq. (1) we can decompose the MSE into a sum of terms involving all the calculated statistical scores, and quantify the contribution of each term to the total error. This decomposition is really useful to understand the source of the difference between the two runs.

$$MSE = (\bar{y} - \bar{o})^2 + \sigma_y^2 + \sigma_o^2 - 2\sigma_y\sigma_o r_{yo} \qquad (1)$$

In our framework, first term in the rhs is the bias between the output of the two simulations. Second term and third term in the rhs are the variances of climSST and eqmeanSST run, respectively. The last term in the rhs accounts for the covariance between climSST and eqmeanSST.

Explained variance

The square of the correlation coefficient in Eq. (2) is an estimate of the amount of the atmospheric variance that can be explained by the SST.

$$r^2 = \frac{Cov^2}{s_y^2 s_o^2} = \frac{EV}{TV} \tag{2}$$

r is the coefficient of correlation between atmospheric fields from climSST and meanSST/eqmeanSST runs. The squared correlation will represent a measure of the extent to which SST variability in different regions can determine the variability of the tropical Atlantic atmosphere. The squared correlation between climSST and meanSST (eqmeanSST) runs gives the atmospheric variance not explained by global (equatorial) SSTs seasonal cycle. In our framework, regions with a higher (lower) squared correlation coefficient are less (more) affected by the seasonal variability in the SST. In summary, the variance explained by SST variability is $(1 - r^2)$ instead of r^2.

Maximum covariance analysis (MCA)

The MCA statistical technique consists of applying the SVD algebraic method to the cross-covariance matrix (R_{SP}) of two fields, S (predictor) and P (predictand) (Suárez-Moreno and Rodríguez-Fonseca 2015). The data matrices S and P need to have the same size in time but the number of elements in space might be different.

$$R_{SP} = S' \cdot P'^T \quad \text{where} \quad S' = S - \langle S \rangle \quad \text{and} \quad P' = P - \langle P \rangle \tag{3}$$

with S' and P' anomalies respect to the annual mean denoted by $\langle \rangle$.

SVD is an algebraic technique to diagonalize non-squared matrices and compute all the components of the eigenvalue problem. Applying it to the cross-covariance matrix we find the matrices U, Q and V that satisfy the relation shown in Eq. (4).

$$R_{SP} = U \cdot Q \cdot V^T \tag{4}$$

The columns (rows) of the matrices U (V^T) are orthogonal and contain the singular vectors of S (P) data matrix. The diagonal matrix Q consists of the singular values $\gamma_k \geq 0$ placed in decreasing order of magnitude. The number of non-zero elements determines the maximum number of each SVD modes we can obtain (Venegas 2001). The evolution in time of the spatial patterns, named as the expansion coefficients, are obtained by projecting each field onto its respective singular vectors as shown in Eq. (5).

$$C_S = U^T \cdot S' \quad C_P = V^T P' \tag{5}$$

Each SVD mode of covariability between S and P is determined by a pair of spatial patterns (one for each field), a pair of expansion coefficients describing the evolution in time of each spatial pattern, and a singular value indicating how much of the squared cross-covariance between the two fields is accounted for by each mode (Storch 1999). Each singular value is proportional to the squared covariance fraction accounted by each mode as shown in Eq. (6).

$$scf_k = \frac{\lambda_k^2}{\sum_i^r \lambda_i^2} \quad \text{with} \quad \lambda_k = \lambda_1, \lambda_2, \dots \lambda_n \tag{6}$$

where k represents the k-th dominant mode and r the chosen truncation limit.

The k-th *homogeneous (heterogeneous) correlation map* (Eqs. 7, 8, respectively) can be constructed as the map of correlation coefficients between the principal component of the corresponding mode k of a field and the values of the same (other) field at each grid point.

$$r[A^k(t), S(t)]; \quad r[B^k(t), P(t)] \tag{7}$$

$$r[A^k(t), P(t)]; \quad r[B^k(t), S(t)] \tag{8}$$

where A and B (see Eqs. 9 and 10) are the principal components of the S and P fields, respectively.

$$A = U^T S \tag{9}$$

$$B = V^T P \tag{10}$$

Lindzen and Nigam mechanism

The Lindzen and Nigam model proposes that low-level winds in the marine atmospheric boundary layer (MABL) are forced by surface temperature gradients. The SST field determines the surface air-temperature resulting in low (high) pressure anomalies, which produce wind convergence (divergence) over warm (cold) SSTs. In this mechanism, the near-surface wind convergence is suggested to be proportional to the Laplacian of the SLP. In particular, Minobe et al. (2008) showed using a MABL model that the momentum equations (Eq. 11) can be reformulated to find that the wind speed convergence is proportional to the Laplacian of the sea level pressure (Eq. 12). In their model the SLP is forced by SSTs following the Eq. (13), so a relationship between SST Laplacian and SLP Laplacian is to be expected.

$$\varepsilon u - fv = \frac{-p_x}{\rho_0}, \quad \varepsilon v + fu = \frac{-p_y}{\rho_0} \tag{11}$$

$$-(u_x + v_y)\rho_0 = \frac{\varepsilon(p_{xx} + p_{yy})}{\varepsilon^2 + f^2} \tag{12}$$

$$\varepsilon p + H(u_x + v_y) = -\gamma T \tag{13}$$

References

Amaya DJ, DeFlorio MJ, Miller AJ, Xie SP (2017) WES feedback and the Atlantic Meridional Mode: observations and CMIP5 comparisons. Clim Dyn 49(5–6):1665–1679

Bjornsson H, Venegas SA (1997) A manual for EOF and SVD analyses of climatic data. CCGCR Rep 97(1):112–134

Chang P, Saravanan R, Ji L, Hegerl GC (2000) The effect of local sea surface temperatures on atmospheric circulation over the tropical atlantic sector. J Clim 13:2195–2216, https://doi.org/10.1175/1520-0442(2000)013%3C2195:TEOLSS%3E2.0.CO;2.

Chelton DB, Esbensen SK, Schlax MG, Thum N, Freilich MH, Wentz FJ, … Schopf PS (2001) Observations of coupling between surface wind stress and sea surface temperature in the eastern tropical Pacific. J Clim 14(7):1479–1498

Chiang JC, Vimont DJ (2004) Analogous Pacific and Atlantic meridional modes of tropical atmosphere–ocean variability. J Clim 17(21):4143–4158

Diakhaté M, Lazar A, De Coëtlogon G, Gaye AT (2018) Do SST gradients drive the monthly climatological surface wind convergence over the tropical Atlantic? Int J Climatol 38:e955–e965

Ding H, Keenlyside NS, Latif M (2009) Seasonal cycle in the upper equatorial Atlantic Ocean. J Geophys Res Oceans 114(C9)

Druyan LM, Fulakeza M (2015) The impact of the Atlantic cold tongue on West African monsoon onset in regional model simulations for 1998–2002. Int J Climatol 35(2):275–287

Frierson DM, Hwang YT (2012) Extratropical influence on ITCZ shifts in slab ocean simulations of global warming. J Clim 25(2):720–733

Gallego D, Ordóñez P, Ribera P, Peña-Ortiz C, García-Herrera R (2015) An instrumental index of the West African Monsoon back to the nineteenth century. Q J R Meteorol Soc 141(693):3166–3176

Gill A (1980) Some simple solutions for heat-induced tropical circulation. Q J R Meteorol Soc 106(449):447–462

Green B, Marshall J (2017) Coupling of trade winds with ocean circulation damps ITCZ shifts. J Clim 30:4395–4411. https://doi.org/10.1175/JCLI-D-16-0818.1

Gu G, Adler RF (2004) Seasonal evolution and variability associated with the West African monsoon system. J Clim 17(17):3364–3377

Hastenrath S (2012) Exploring the climate problems of Brazil's Nordeste: a review. Clim Change 112(2):243–251

Huffman GJ, Adler RF, Bolvin DT, Gu GJ, Nelkin EJ, Bowman KP, Hong Y, Stocker EF, Wolff DB (2007) The TRMM multisatellite precipitation analysis (TMPA): Quasi-global, multiyear, combined sensor precipitation estimates at fine Scales. J Hydrometeorol 8:38–55

Kang SM, Held IM, Frierson DM, Zhao M (2008) The response of the ITCZ to extratropical thermal forcing: Idealized slab-ocean experiments with a GCM. J Clim 21(14):3521–3532

Kang SM, Frierson DM, Held IM (2009) The tropical response to extratropical thermal forcing in an idealized GCM: The importance of radiative feedbacks and convective parameterization. J Atmos Sci 66(9):2812–2827

Keenlyside N, Latif M (2007) Understanding equatorial Atlantic interannual variability. J Clim 20(1):131–142. https://doi.org/10.1175/JCLI3992.1

Kobayashi S, Ota Y, Harada Y, Ebita A, Moriya M, Onoda H, Onogi K, Kamahori H, Kobayashi C, Endo H, Miyaoka K, Takahashi K (2015) The JRA-55 reanalysis: general specifications and basic characteristics. J Meteorol Soc Jpn 93:5–48. https://doi.org/10.2151/jmsj.2015-001

Koseki S, Koh T-Y, Teo C-K (2013) Effects of the cold tongue in the South China Sea on the monsoon, diurnal cycle and rainfall in the Maritime Continent. Q J R Meteorol Soc 139(675):1566–1582. https://doi.org/10.1002/qj2025

Koseki S, Keenlyside N, Demissie T, Toniazzo T, Counillon F, Bethke I, Iliack M, Shen M-L (2017) Causes of the large warm bias in the Angola-Benguela Frontal Zone in the Norwegian Earth System Model. Clim Dyn. https://doi.org/10.1007/s00382-017-3896-2

Li T, Philander SGH (1997) On the seasonal cycle of the equatorial Atlantic Ocean. J Clim 10(4):813–817

Lindzen RS, Nigam S (1987) On the role of sea surface temperature gradients in forcing low-level winds and convergence in the tropics. J Atmos Sci 44(17):2418–2436

Lumpkin R, Speer K (2007) Global ocean meridional overturning. J Phys Oceanogr 37(10):2550–2562

Marshall J, Donohoe A, Ferreira D, McGee D (2014) The ocean's role in setting the mean position of the Inter-Tropical convergence zone. Clim Dyn 42(7–8):1967–1979

Mechoso CR, Losada T, Koseki S, Mohino-Harris E, Keenlyside N, Castaño-Tierno A et al (2016) Can reducing the incoming energy flux over the Southern Ocean in a CGCM improve its simulation of tropical climate? Geophys Res Lett 43:11057–11063. https://doi.org/10.1002/2016GL071150

Meynadier R, de Coëtlogon G, Leduc-Leballeur M, Eymard L, Janicot S (2016) Seasonal influence of the sea surface temperature on the low atmospheric circulation and precipitation in the eastern equatorial Atlantic. Clim Dyn 47: 1127–1142. https://doi.org/10.1007/s00382-015-2892-7

Minobe S, Kuwano-Yoshida A, Komori N, Xie SP, Small RJ (2008) Influence of the Gulf Stream on the troposphere. Nature 452(7184):206–209

Mitchell TP, Wallace JM (1992) The annual cycle in equatorial convection and sea surface temperature. J Clim 5(10):1140–1156

Mohino E, Rodríguez-Fonseca B, Losada T, Gervois S, Janicot S, Bader J et al (2011) Changes in the interannual SST-forced signals on West African rainfall. AGCM intercomparison. Clim Dyn 37(9–10):1707–1725

Moore D, Hisard P, McCreary J, Merle J, O'Brien J, Picaut J, … Wunsch C (1978) Equatorial adjustment in the eastern Atlantic. Geophys Res Lett 5(8):637–640

Murphy AH, Winkler RL (1987) A general framework for forecast verification. Mon Weather Rev 115(7):1330–1338

Neale RB, Richter J, Park S, Lauritzen PH, Vavrus SJ, Rasch PJ, Zhang M (2013) The mean climate of the Community Atmosphere Model (CAM4) in forced SST and fully coupled experiments. J Clim 26(14):5150–5168

Okumura Y, Xie SP (2004) Interaction of the Atlantic equatorial cold tongue and the African monsoon. J Clim 17(18):3589–3602

Philander SGH, Pacanowski RC (1986) A model of the seasonal cycle in the tropical Atlantic Ocean. J Geophys Res 91(C12):14192–14206. https://doi.org/10.1029/JC091iC12p14192

Philander SGH, Gu D, Lambert G, Li T, Halpern D, Lau NC, Pacanowski RC (1996) Why the ITCZ is mostly north of the equator. J Clim 9(12):2958–2972

Reynolds RW, Smith TM, Liu C, Chelton DB, Casey KS, Schlax MG (2007) Daily high-resolution-blended analyses for sea surface temperature. J Clim 20(22):5473–5496

Richter I (2015) Climate model biases in the eastern tropical oceans: causes, impacts and ways forward. Wiley Interdiscip Rev Clim Change 6(3):345–358

Richter I, Behera SK, Doi T, Taguchi B, Masumoto Y, Xie SP (2014) What controls equatorial Atlantic winds in boreal spring? Clim Dyn 43(11):3091–3104

Saravanan R, Chang P (1999) Oceanic mixed layer feedback and tropical Atlantic variability. Geophys Res Lett 26(24):3629–3632

Saravanan R, Chang P (2004) Thermodynamic coupling and predictability of tropical sea surface temperature. Thermodynamic coupling and predictability of tropical sea surface temperature.

Earth's Climate: The Ocean-Atmosphere Interactio. In: Wang C, Xie S-P, Carton J (eds) Geophysical Monograph Series, American Geophysical Union, Washington, pp 171–180

Schneider T, Bischoff T, Haug GH (2014) Migrations and dynamics of the intertropical convergence zone. Nature 513(7516):45–53

Suárez-Moreno R, Rodríguez-Fonseca B (2015) S4CAST v2.0: sea surface temperature based statistical seasonal forecast model. Geosci Model Dev 8:3639–3658. https://doi.org/10.5194/gmd-8-3639-2015

Takatama K, Minobe S, Inatsu M, Small RJ (2012) Diagnostics for near-surface wind convergence/divergence response to the Gulf Stream in a regional atmospheric model. Atmos Sci Lett 13(1):16–21

Venegas SA (2001) Statistical methods for signal detection in climate. Danish Center Earth Syst Sci Rep 2:96

von Storch H, Navarra A (1995) Analysis of Climate Variability, Springer-Verlag, New York, pp 334

Wallace JM, Mitchell TP, Deser C (1989) The influence of sea-surface temperature on surface wind in the eastern equatorial Pacific: Seasonal and interannual variability. J Clim 2(12):1492–1499

Wilks DS (2011) Statistical methods in the atmospheric sciences, vol 100. Academic Press, New York

Xie S (1999) A dynamic ocean–atmosphere model of the tropical Atlantic decadal variability. J Clim 12:64–70. https://doi.org/10.1175/1520-0442(1999)012%3C0064:ADOAMO%3E2.0.CO;2

Zebiak SE (1993) Air–sea interaction in the equatorial Atlantic region. J Clim 6:1567–1586. https://doi.org/10.1175/1520-0442(1993)006%3C1567:AIITEA%3E2.0.CO;2.

Zermeño-Diaz DM, Zhang C (2013) Possible root causes of surface westerly biases over the equatorial Atlantic in global climate models. J Clim 26(20):8154–8168

Zhang R, Delworth TL (2005) Simulated tropical response to a substantial weakening of the Atlantic thermohaline circulation. J Clim 18(12):1853–1860

Zhang GJ, McFarlane NA (1995) Role of convective scale momentum transport in climate simulation. J Geophys Res 100(D1):1417–1426. https://doi.org/10.1029/94JD02519